Bioorganic Chemistry 96 (2020) 103621

Contents lists available at ScienceDirect

Bioorganic Chemistry

journal homepage: www.elsevier.com/locate/bioorg

Synthesis and *in vitro* investigation of novel cytotoxic pyrimidine and pyrazolopyrimidne derivatives showing apoptotic effect

Fatma A. Ragab[a,*], Yassin M. Nissan[a,b], Emad M. Seif[b,*], Ahmed Maher[c], Reem K. Arafa[d]

[a] Pharmaceutical Chemistry Department, Faculty of Pharmacy, Cairo University, Kasr Elini St., Cairo 11562, Egypt
[b] Pharmaceutical Chemistry Department, Faculty of Pharmacy, October University for Modern Sciences and Arts (MSA), Giza, Egypt
[c] Biochemistry Department, Faculty of Pharmacy, October University for Modern Sciences and Arts (MSA), Giza, Egypt
[d] Biomedical Sciences Program, University of Science and Technology, Zewail City of Science and Technology, 12578 Cairo, Egypt

ARTICLE INFO

Keywords:
Pyrimidine based hybrids
Pyrazolopyrimidine hybrids
Cytotoxicity
Apoptosis

ABSTRACT

A series of novel derivatives of hydrazinylpyrimidines, pyrazolylpyrimidines and 3-amino[3,4-*d*]pyrazolopyrimidines have been synthesized and tested for their *in vitro* cytotoxic activity against 60 tumor cell lines by NCI. The *in vitro* cytotoxic IC_{50} values for the most active compounds were determined against the colon-KM12 cell line (**5d**, **7c** and **7d**), breast-MCF-7 (**6a**) and melanoma-MDA-MB-435 (**6h**) using 5-fluorouracil (5-FU) as a positive control. Derivatives **5d** and **7c** were found to be the most potent derivatives against KM12 cell line (IC_{50} = 1.73 and 1.21 μM, respectively) with a high selectivity index (SI) (18.82 and 35.49, respectively) compared to 5-FU (IC_{50} = 12.26 μM, SI = 1.93). Compounds **5d** and **7c** were further investigated for their apoptotic behavior in KM12 cell line. The investigations showed the up-regulation of caspase 3/9 and the pro-apoptotic factor Bax. On the other hand, the expression of the anti-apoptotic factor Bcl-2, was down-regulated, as well as its inhibition at a nanomolar concentration. Furthermore, the apoptotic effect for derivatives **5d** and **7c** in KM12 cells was detected using annexin V-FITC staining method.

1. Introduction

Inhibition of cell cycle progression and induction of apoptosis represent a key strategy for prevention and treatment of cancer [1]. Apoptosis or programmed cell death is considered a natural process in elimination of any unneeded or abnormal cells [1,2]. Two major pathways of apoptosis have been identified; the intrinsic (mitochondrial mediated) pathway which is regulated by Bcl-2 family and extrinsic (death receptor mediated) pathway which is regulated by a subgroup of tumor necrosis factor receptors superfamily (TNFR) [3]. Instantly as apoptosis process is initiated, caspases, a family of cysteine proteases, are activated. Caspases are subdivided into initiator caspases as caspases 2, 8 and 9, effector caspases as caspases 3, 6 and 7 and inflammatory caspases as caspases 1, 4, 5, 11 and 12 [3]. Caspase 9 is the initiator of the intrinsic apoptosis while caspase 8 is the initiator of the extrinsic apoptosis. Caspases 8 and 9 activate the effector caspases 3 and 7 which trigger apoptosis. Diverse anticancer drugs act by induction of apoptosis [4–8]. Cancer cells can avoid apoptosis by hindering caspase function, decreasing Bax expression level or increasing gene expression level of anti-apoptotic Bcl-2 [2]. Apoptosis process could be induced by death receptors agonists, DNA damage, mitotic spindle dysfunction and cell cycle progression disturbance [9,10].

One of the most important building blocks of nucleic acids is the pyrimidine ring, subsequently its derivatives possess a diverse chemotherapeutic profile as antimicrobial, antiviral or anticancer activity [11,12]. Among these reported pharmacological activities of pyrimidine based scaffolds, antitumor activity is the most widely reported [11–19]. The antiproliferating activity of the pyrimidine based scaffold is owing to their ability to bind with several enzymes, receptors and target proteins (Fig. 1) [20]. 5-Fluoruracil is a dihydropyrimidine derivative used in the treatment of various types of cancer as metastatic colorectal, colon, nasopharyngeal and breast cancer and acts through irreversible inhibition of thymidylate synthase [21,22]. 5-FU induce varying degrees of apoptosis in colorectal cancer cells by the activation of caspase-9 [23] and is known to affect the cell cycle [24]. Monastrol is another dihydropyrimidine derivative inhibits the motility of the mitotic kinesin Eg5 and arrest the cell cycle at G2/M phase [25]. In addition, several pyrimidin-5-carbonitrile derivatives as **I** and **II** exhibit cytotoxic activity against wide range of cancer cell lines [26–34]. Moreover, several bicyclic condensed pyrimidines possess antitumor activity by inhibiting different protein kinases. On the other hand, pyrazoles demonstrate a great potential in the design of anticancer

* Corresponding authors.
E-mail address: ph.emad.seif@gmail.com (E.M. Seif).

https://doi.org/10.1016/j.bioorg.2020.103621
Received 10 October 2019; Received in revised form 1 January 2020; Accepted 22 January 2020
Available online 24 January 2020

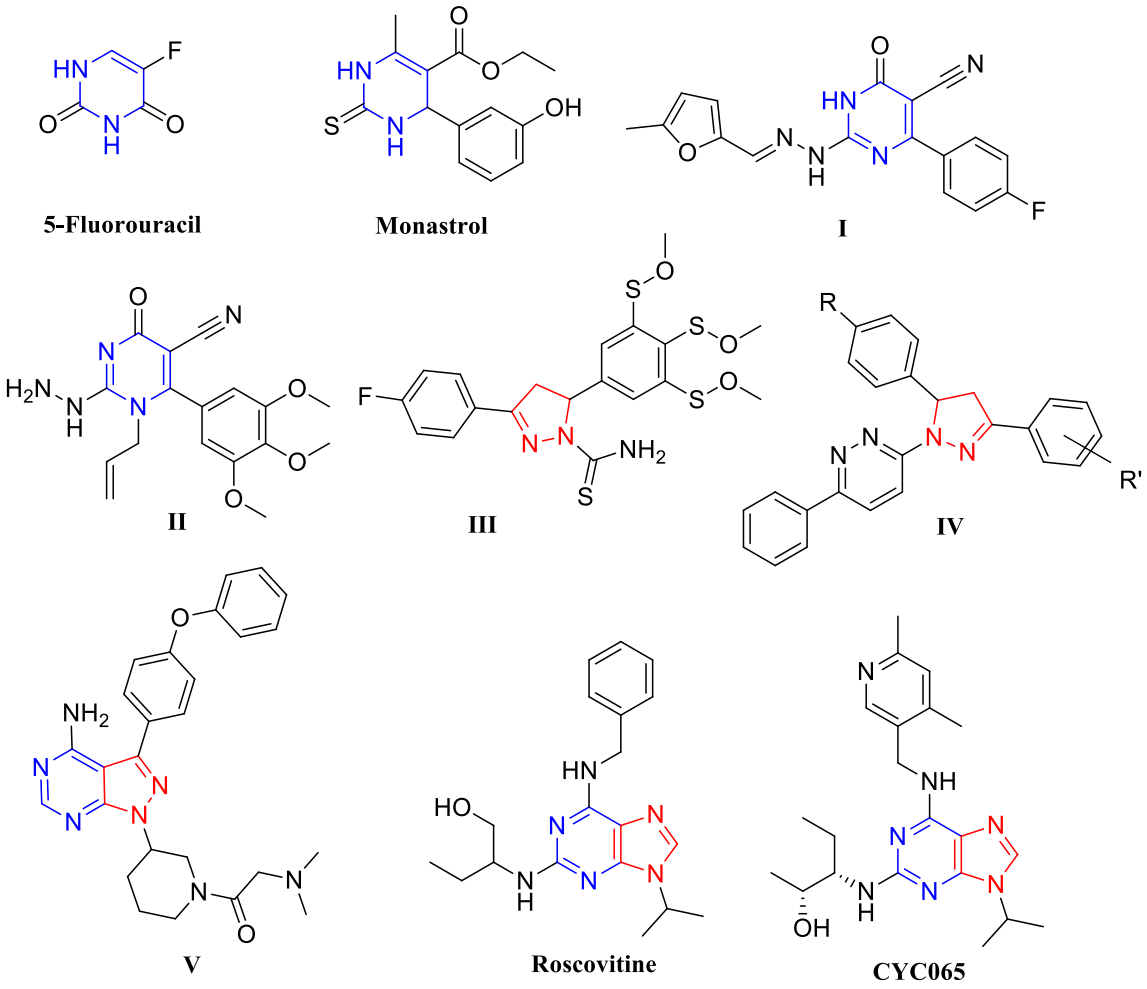

Fig. 1. Biologically active pyrimidine, pyrazoline and fused pyrimidine derivatives with anticancer activity.

agents and also stimulate activity of proapoptotic proteins [35–37]. Furthermore, dihydropyrazoles act as selective inhibitors for EGFR and/or Her-2 and telomerase enzyme which are useful targets for cancer treatment [38–40]. Some pyrazoline derivatives as **III** and **IV** inhibit also the proliferation of some types of cancer through inhibition of cell cycle progression and induction of apoptosis through upregulation of caspase 3 and Bax expression level [41,42]. Pyrazolopyrimidines as Roscovitine, CYC065 and **V,** bioisosteres of adenine, act as apoptotic inducers through elevation of caspase 3 level and cell cycle arrest at G1, S and G2/M phases (Fig. 1) [43–46].

Consequently, the present investigation describes the synthesis of new pyrimidine derivatives (**5a-d**) and pyrimidine based hybrids molecules containing fused (**7a-d** and **8a-f**) and non-fused (**6a-h**) pyrazole moiety to be tested as anticancer agents (Fig. 2).

2. Results and discussion

2.1. Chemistry

The key starting dihydropyrimidines **1a** and **1b** have been synthesized according to the reported method involving cyclocondensation of thiourea, furan-2-carboxaldehyde or 2-thiophenecarboxaldehyde, respectively with ethylcyanoacetate in anhydrous K_2CO_3/ethanol [47]. Hydrazinolysis of **1a** and **1b** afforded 2-hydrazino derivatives **2a** and **2b**, respectively [48,49]. Regioselective methylation of **1a** and **1b** with methyl iodide in DMF at 0 °C in presence of K_2CO_3 yielded the S-methyl derivatives **3a** and **3b**, respectively [50]. Reaction of **1a**, **1b**, **3a** and **3b** with a mixture of phosphorous oxychloride and phosphorous pentachloride gave the corresponding chloro derivatives **4a-d** [50,51]. The

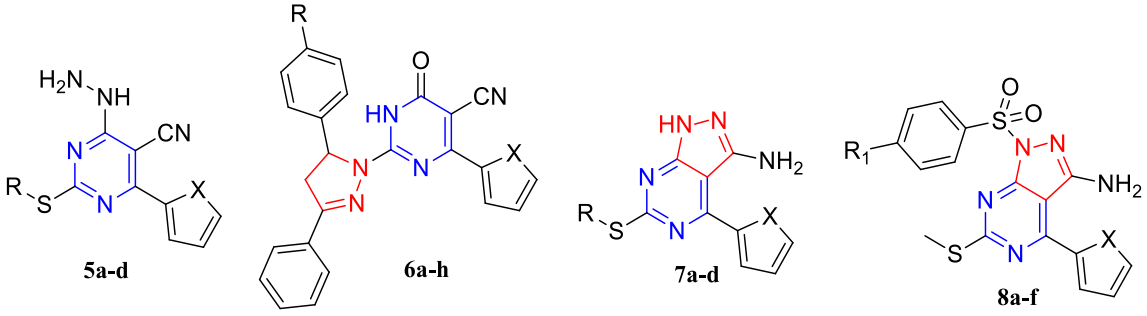

Fig. 2. The targeted compounds **5a-d**, **6a-h**, **7a-d** and **8a-f.**

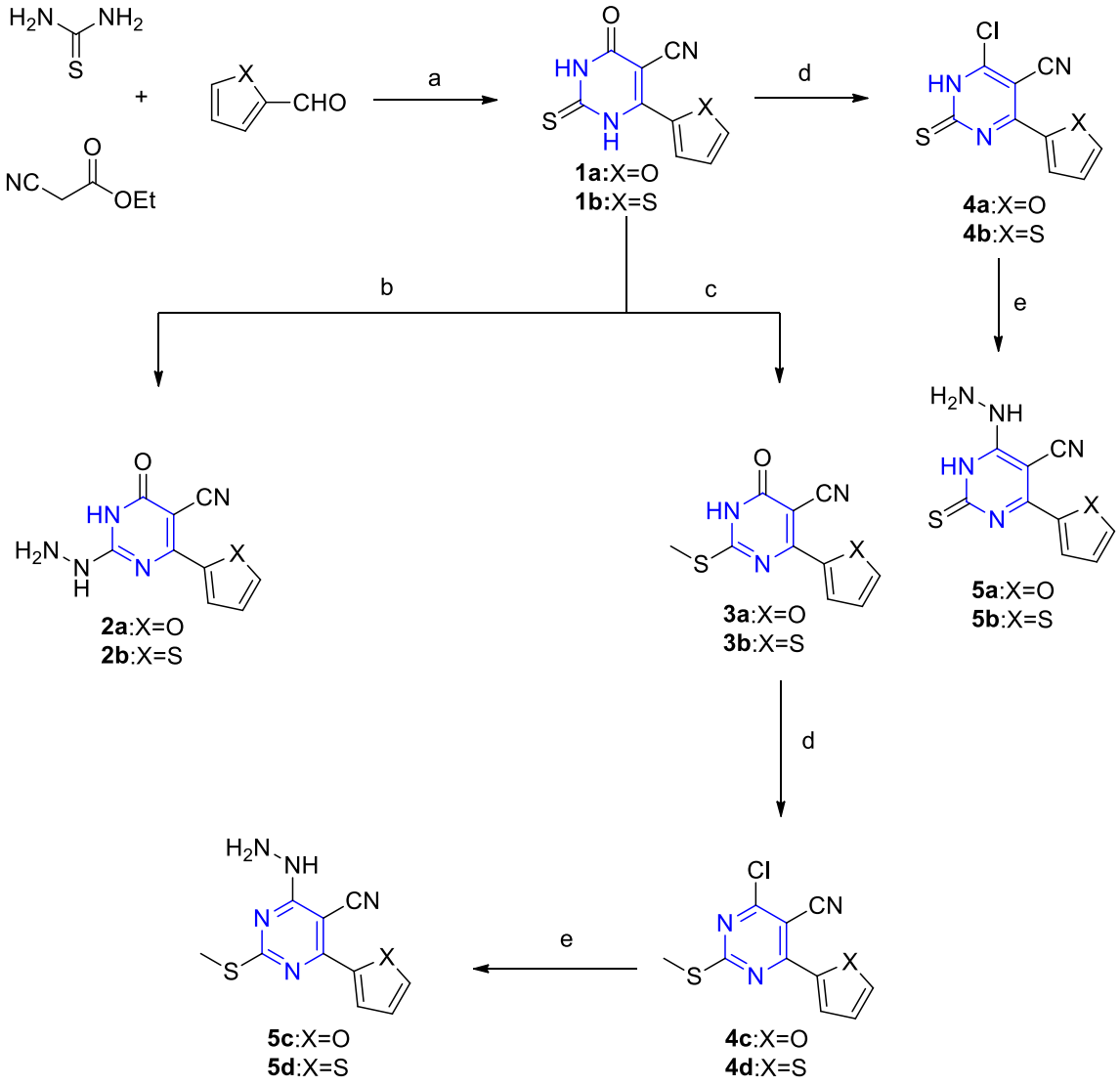

Scheme 1. Reagets and conditions: (a) K_2CO_3, abs. ethanol, reflux 12 h: (b) NH_2NH_2, methanol, reflux 12 h: (c) MeI, DMF, Ice bath, 3 h: (d) $POCl_3$, PCl_5, reflux 30 h: (e) NH_2NH_2, Methanol, rt, 5 h.

structure of **4b** was confirmed by IR, which showed bands at 3440 cm^{-1} (NH) and 2228 cm^{-1} (CN). ^1H NMR of **4b** showed three signals attributed to thiophene protons at δ 7.30, 7.98, 8.08 ppm and a singlet at δ 11.81 ppm (NH-exchangeable with D_2O). The chloro derivatives **4a-d** were reacted with hydrazine hydrate at room temperature to give the hydrazino derivatives **5a-d** (Scheme 1). IR spectra of derivatives **5a-d** revealed bands at 3350–3309 cm^{-1} (NH, NH_2).

Reaction of the hydrazino derivatives **2a** and **2b** with various chalcones yielded the cyclic pyrazoline derivatives **6a-h** (Scheme 2). The IR spectra of **6a-h** derivatives exhibited bands at 3436–3363 cm^{-1} (NH of pyrimidine) and at 1658–1644 cm^{-1} (C═O). ^1H NMR spectra showed the characteristic AMX prominent pattern of pyrazoline protons where C4-H_A, H_M and C5-H_X appeared as doublet of doublet signals at δ 3.17–3.40, 3.95–4.01 and 5.74–5.79 ppm, respectively. Besides exchangeable NH pyrimidine singlet signals appeared at δ 12.27–13.43 ppm. ^{13}C NMR spectra elucidated C4 and C5 of pyrazoline at δ 40.42–40.62 and δ 55.64–62.34 ppm, respectively (Scheme 2).

The pyrazolopyrimidine derivatives **7a-d** were obtained through intramolecular cyclization of hydrazino derivatives **5a-d**. Reaction of **7c** and **7d** with *p*-substituted arylsulfonyl chlorides yielded the phenyl sulfonyl pyrazolopyrimidine derivatives **8a-f**.

IR of **7a-d** was characterized by absence of CN band. ^1H NMR of **7a-d** showed a singlet signal at δ 5.35–5.92 ppm (NH_2) in addition to a singlet signals at δ 12.27–12.77 (NH pyrazole exchangeable with D_2O). IR spectra of **8a-f** showed bands at 3495–3286 (NH_2) while ^1H NMR spectra showed singlet signals at δ 2.65–2.66 (SCH_3) and at δ 6.00–6.60 (NH_2) (Scheme 3).

2.2. Biological evaluation

2.2.1. Antiproliferative activity

The synthesized compounds were chosen and tested for their *in vitro* antiproliferative activity by the National Cancer Institute (NCI), Germantown MD, USA, under the Development Therapeutic Program (DTP) on a panel of 60 tumor cell lines representing breast, CNS, colon, leukemia, melanoma, non-small cell lung, ovarian, prostate and renal cancers. The compounds were screened in an initial one dose at conc. 10 μM and results are presented as percent growth inhibition of the treated cells (GI %) (As seen in supplementary data).

With regards to the cytotoxicity against the breast cancer cell line (MCF-7), the unsubstituted derivative **6a** was the most active (GI % = 59.97) while the para fluoro derivative **6c** and para methoxy derivative **6d** showed a little less cytotoxic activity (GI % of 47.43 and 33.97, respectively). The thiophene derivatives **6e**, **6g** and **6h** displayed significant less cytotoxic activity (GI % = 23.63, 22.50 and 23.82).

With respect to the colon cancer cell line (KM12), three derivatives

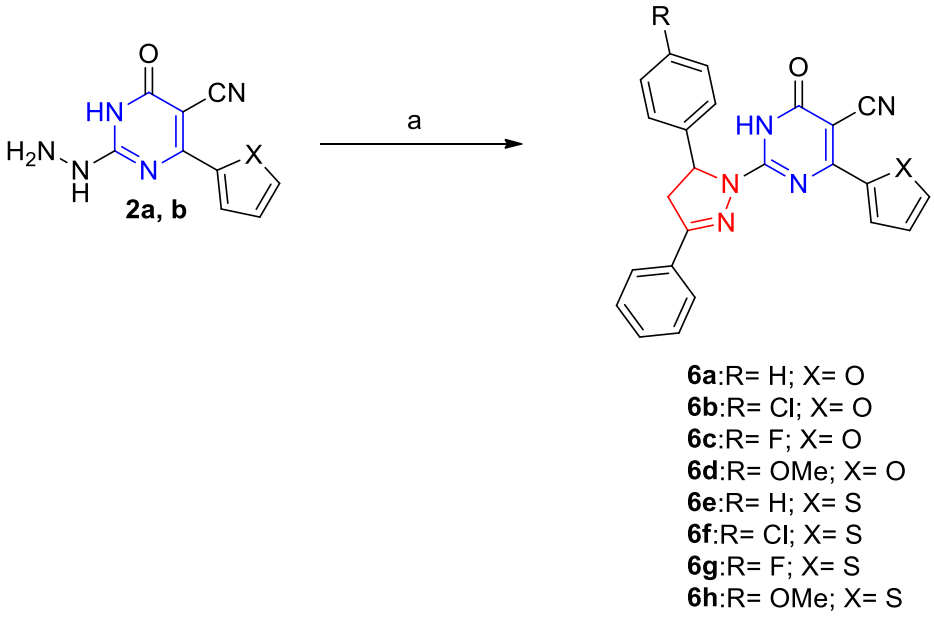

Scheme 2. Reagets and conditions: (a) chalocones, abs ethanol, NaOH, reflux, 70 h.

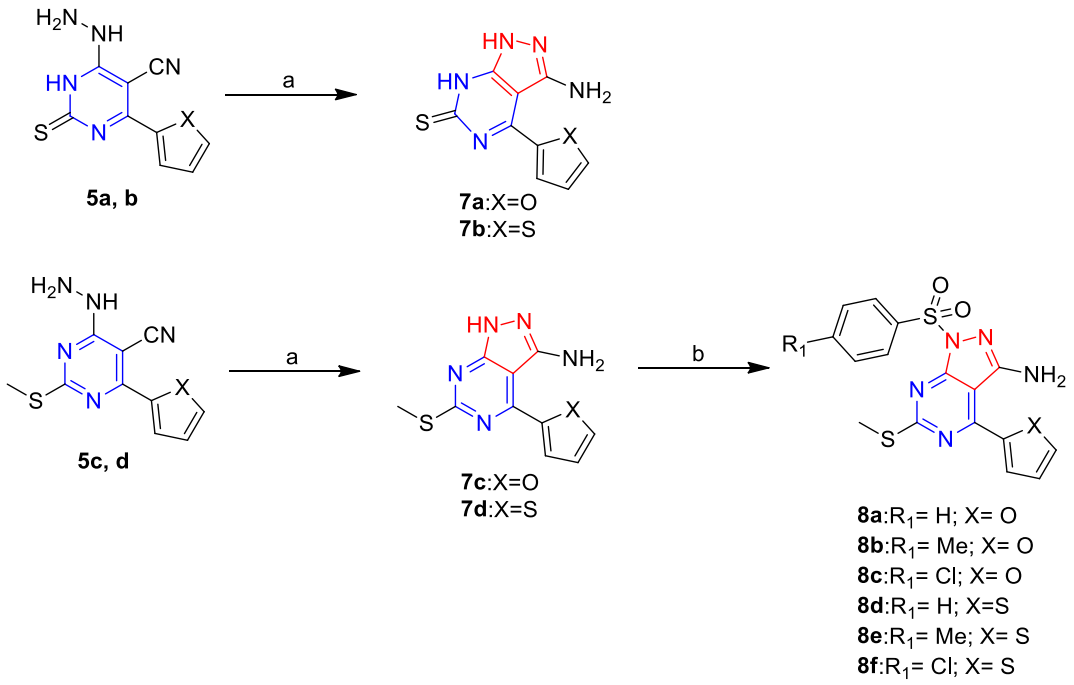

Scheme 3. Reagets and conditions: (a) abs ethanol, conc. HCl, reflux, 12 h: (b) arylsulfonyl chloride derivatives, dry pyridine, reflux, 8 h.

5d, **7c** and **7d** exhibited good potency with GI % = 57.94, 55.93 and 51.22, respectively. In the series of the hydrazino derivatives **5a-d**, it was noticed that the thiomethyl derivatives **5c** (GI % = 33.16) and **5d** (GI % = 57.94) were more potent against colon cancer cell line (KM12) than thioxo derivatives **5a** (GI % = 0.27) and **5b** (GI % = 6.51), respectively.

Furthermore, the fused pyrazolopyrimidine derivative **7c** and **7d** exhibited high potency (GI% = 55.93 and 51.22, respectively) when compared to the desmethyl analogs **7a** and **7b** (GI% less than 20)

Referring to melanoma (MDA-MB-435) cancer cell line, the only active derivative was **6h** (GI % = 55.30) (Fig. 3).

2.2.2. *In vitro* IC_{50} evaluation

The *in vitro* cytotoxic IC_{50} values of the most active derivatives in the NCI growth inhibition assay **5d**, **6a**, **6h**, **7c** and **7d** were determined against the most sensitive cancer cell lines viz. colon (KM12), breast (MCF-7) and melanoma (MDA-MB-435) and against the corresponding normal colon (FHC), breast (MCF10a) and skin (HFB4) cell lines using 5-fluorouracil as a positive control (Table 1).

Compounds **5d**, **7c** and **7d** were more potent against KM12 cell line (IC_{50} = 1.73, 1.21 and 5.55 μM, respectively) with higher selectivity index (SI) (18.82, 35.49 and 2.49, respectively) than 5-FU (IC_{50} = 12.26 μM, SI = 1.93). Compound **6a** showed potent activity against MCF-7 cell line (IC_{50} = 4.22 μM) with high SI (21.50) although lower than 5-FU (IC_{50} = 2.44 μM and SI = 43.21). Compound **6h** also exhibited remarkable activity against MDA-MB-435 cells (IC_{50} = 5.25 μM, SI = 8.42) but still lower than 5-FU (IC_{50} = 2.52 μM, SI = 14.08).

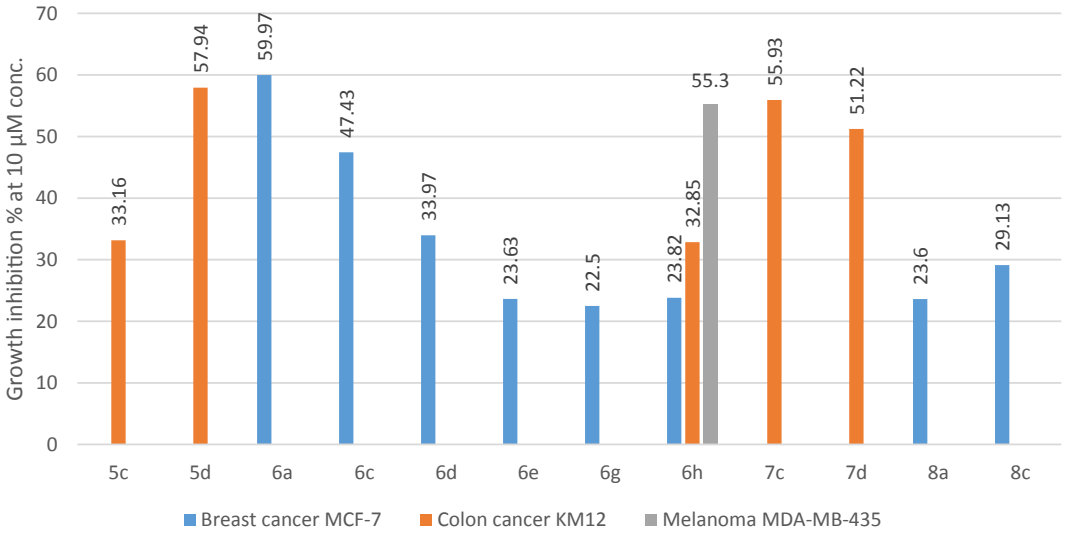

Fig. 3. Growth inhibition percentage of the tested compounds exceeding 20% at 10 µM concentration in MCF-7, KM12 and MDA-MB-435 cell lines.

2.2.3. Caspase 3/9 assay

Compounds **5d** and **7c** were selected for further evaluation of their caspase activation ability in colon cancer cell line (KM12). They showed significant increase in the cellular levels of both caspase 3 (0.5217 and 0.5951 ng/mL, respectively) and caspase 9 (14.77 and 18.45 ng/mL, respectively) compared to untreated cells (caspase 3 = 0.04316 ng/mL and caspase 9 = 0.91 ng/mL) (Table 2).

2.2.4. Evaluation of Bax and Bcl-2 expressions

Bax and Bcl-2 cellular levels were assayed for **5d** and **7c** in colon (KM12) cells. The gene expression fold values were presented in Table 3. Results showed an increase of the pro-apoptotic factor Bax by 6.50 and 6.07 folds, respectively while anti-apoptotic protein Bcl-2 demonstrated a concentration decrease by 0.29 and 0.35 folds, respectively.

2.2.5. In vitro Bcl-2 inhibition assay

Bcl-2 anti-apoptotic protein, a member of Bcl-2 family, is an attractive target in cancer therapy where the ability of the cancer cells to survive and resist apoptosis is closely related to the high expression level of Bcl-2 protein [52,53]. In a trial for further investigation of the apoptotic induction mechanism exhibited by **5d** and **7c**, *in vitro* Bcl-2 inhibition assay was performed using venetoclax as a reference. Venetoclax is a selective Bcl-2 inhibitor used in the treatment of chronic lymphocytic leukeamia (CLL). It restores the normal apoptosis process in malignant cells through liberating the pro-apoptotic factors from Bcl-2 [54].

Fortunately, both compounds showed inhibitory action at nanomolar level (IC_{50} = 852.78 and 449.42 nM, respectively) towards the evaluated protein. These results may add an extra mechanism of action for the newly synthesized compounds and contribute to their apoptotic behavior in cancer cells (Table 4).

2.2.6. Cell cycle analysis

To further investigate the apoptotic capacity of **5d** and **7c**, flow-cytometric analysis was performed on colon (KM12) cancer cell line treated with the tested compounds at their IC_{50} concentrations using untreated colon (KM12) cancer cells as a negative control. There was an elevation of apoptotic cells at pre-G1 phase (14.36% and 22.81%, respectively) compared to control KM12 cells (2.16%) as well as an

Table 1
IC_{50} values of the MTT assayed compounds against the most sensitive cell lines.

Compound #	IC_{50} results (µM)*					
	Cancer cell lines			Normal cell lines		
	MCF7	MDA-MB-435	KM12	MCF10a	HFB4	FHC
5d	NT**	NT	1.73 ± 0.06 SI = 18.82***	NT	NT	32.57 ± 1.97
6a	4.22 ± 0.31 SI = 21.50	NT	NT	90.74 ± 6.8	NT	NT
6h	NT	5.25 ± 0.24 SI = 8.42	NT	NT	44.25 ± 2.1	NT
7c	NT	NT	1.21 ± 0.04 SI = 35.49	NT	NT	42.95 ± 2.55
7d	NT	NT	5.55 ± 0.31 SI = 2.49	NT	NT	13.87 ± 1.74
5-FU	2.44 ± 0.23 SI = 43.21	2.52 ± 0.12 SI = 14.08	12.26 ± 1.4 SI = 1.93	105.45 ± 7.22	35.5 ± 1.9	23.78 ± 1.5

* IC_{50} values are the average of 3 independent runs ± SD.
** NT = not tested.
*** SI = selectivity index.

Table 2
Caspase 3/9 concentrations in treated KM12 cells with **5d** and **7c**.

Compound #	Caspase 3 (ng/mL)*	Caspase 9 (ng/mL)*
5d	0.5217 ± 21.1	14.77 ± 0.83
7c	0.5951 ± 18.3	18.45 ± 1.21
Control	0.04316 ± 3.42	0.91 ± 0.04

* Data are presented as the mean of 3 independent runs ± SD.

Table 3
Bax and Bcl-2 expression levels in treated KM12 cells with **5d** and **7c**.

Compound #	Pro-apoptotic Bax (fold)*	Anti-apoptotic Bcl-2 (fold)
5d	6.50	0.29
7c	6.07	0.35
Control	1.00	1.00

Table 4
Bcl-2 inihibtion assay of **5d** and **7c.**

Compound #	Bcl-2 IC_{50} (nM)
5d	852.78 ± 24.5
7c	449.42 ± 13.01
venetoclax	202.01 ± 7.32

accumulation of cells at the G2-M phase (34.28% and 42.08%, respectively) versus control KM12 cells (11.19%). On the contrary, the percentage of treated cells in G0/G1 phase was reduced (44.15% and 35.28%, respectively) compared to untreated cells (55.48%) also in S phase the percentage of treated cells was reduced (21.57% and 22.64%, respectively) compared to untreated cells (33.33%) (Fig. 4 and Table 5).

2.2.7. Apoptotic cells sub-population determination

To support the fact that derivatives **5d** and **7c** induce apoptosis in colon (KM12) cancer cell line, annexin V-FITC and propidium iodide double staining method was used. Table 6 displays the percentage of early and late apoptotic populations as well as the necrotic population relative to the total apoptotic cells. When KM12 cells were treated with the IC_{50} dose of compounds **5d** and **7c**, the percentage of early and late apoptotic populations increased from 1.31% and 0.26%, respectively in control untreated cells to 6.77% and 6.05%, respectively in **5d** treated cells and to 5.92% and 13.6%, respectively in **7c** treated cells. This proves that the antiproliferative effect is associated with a pro-apoptotic activity of the tested compounds (Fig. 5).

Table 5
Cell cycle analysis in treated KM12 cells with **5d** and **7c**.

Compound #	% G0-G1*	%S*	%G2-M*	%Pre-G1 apoptosis*
5d	44.15 ± 2.82	21.57 ± 1.92	34.28 ± 1.86	14.36 ± 1.1
7c	35.28 ± 2.36	22.64 ± 1.73	42.08 ± 3.17	22.81 ± 2.5
Control	55.48 ± 3.71	33.33 ± 2.36	11.19 ± 1.24	2.16 ± 0.22

* Data are presented as the mean of 3 independent runs ± SD.

Table 6
Apoptotic cells sub-population percentage in treated KM12 cells with **5d** and **7c**.

Compound #	Total*	Early*	Late*	Necrosis*
5d	14.36 ± 0.88	6.77 ± 0.34	6.05 ± 0.33	1.54 ± 0.65
7c	22.81 ± 2.11	5.92 ± 0.29	13.6 ± 1.21	3.29 ± 0.19
Control	2.16 ± 0.13	1.31 ± 0.07	0.26 ± 0.04	0.59 ± 0.03

* Data are presented as the mean of 3 independent runs ± SD.

2.3. Molecular docking

Docking studies of **5d** and **7c** in the BH3 groove of Bcl-2 were performed to predict the binding mode of interactions between the synthesized derivatives and the active site. Both the co-crystallized ligand **398** and the reference drug **venetoclax** were also docked using the same protocol of **5d** and **7c** docking process for validation (Table 7). The docked pose of **398** (RMSD < 1) and **venetoclax** showed interaction with Tyr 67 (1 hydrogen bond; 1.97 Å) and Arg 105 (2 hydrogen bonds; 1.98 and 2.67 Å), respectively (Fig. 6).

Investigational analysis of the predicted binding modes of **5d** and **7c** helps their assumed direct inhibitory role where **5d** form two hydrogen bonds with Arg 105 residue (2.13 and 2.38 Å) and **7c** form single hydrogen bond with Tyr 161 (2.35 Å) residue in the active site (Fig. 7).

3. Conclusions

Three series of hydrazinopyrimidines **2a**, **b** and **5a-d**, 2-pyrazolylpyrimidines **6a-h**, and 3-amino[3,4-*d*]pyrazolopyrimidines **7a-d** and **8a-f** have been synthesized and tested for their *in vitro* cytotoxic activity against 60 tumor cell lines by NCI. In vitro IC_{50} determination of the best five derivatives were determined against cancer and normal cell lines. Compounds **5d** and **7c** were found to be the most potent and selective derivatives against KM12 cell line. Caspase activation assay was performed for both **5d** and **7c** derivatives in colon (KM12) cancer cell line. The results showed significant increase of caspase 3 (0.5217 and 0.5951 ng/mL, respectively) and caspase 9 (14.77 and 18.45 ng/mL, respectively) compared to untreated KM12 (0.04316 and 0.91 ng/mL, respectively). Bax and Bcl-2 concentration levels were also evaluated and showed a titer increase of the pro-apoptotic protein Bax (6.50

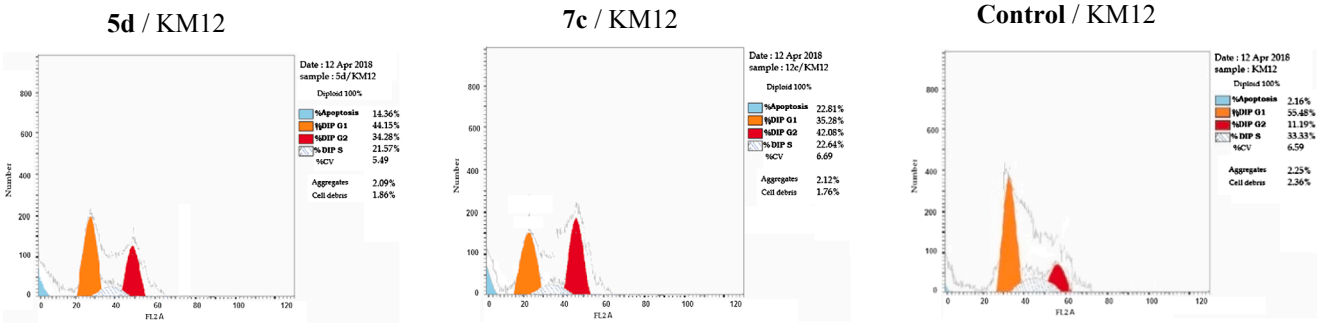

Fig. 4. Effect of **5d** and **7c** on the cell cycle of KM12 cells.

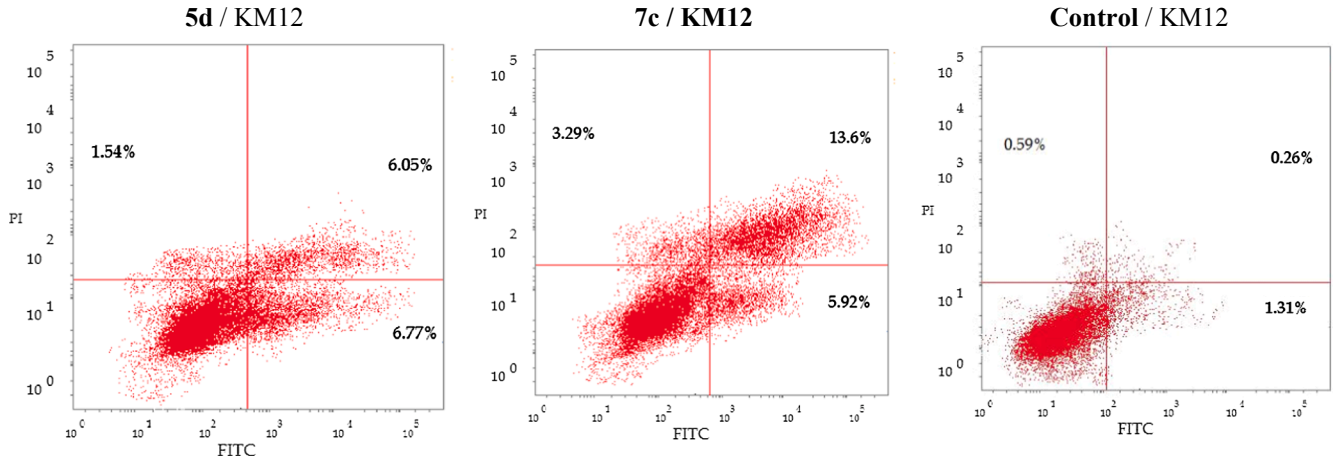

Fig. 5. Effect of **5d** and **7c** on the percentage of annexin V-FITC-positive staining in KM12 cells.

Table 7
Docking scores of **5d** and **7c** in the active site of Bcl-2 [PDB ID: 4AQ3].

Compound #	Docking score (Kcal/mol)
5d	−5.4
7c	−5.6
Co-crystallized ligand (398)	−11.1
venetoclax	−9.4

and 6.07 fold, respectively) and a decrease of the anti-apoptotic protein Bcl-2 (0.29 and 0.35 fold, respectively) compared to untreated KM12 cells, thus confirming their involvement in apoptosis induction. In vitro Bcl-2 inhibition assay was performed for compounds **5d** and **7c** to confirm their apoptotic activity. Compound **7c** showed Bcl-2 inhibition with IC_{50} = 449.42 nM. Furthermore, flow cytometric assay results showed that the apoptotic cells percentage was significantly elevated at the pre-G1 phase to 14.36% and 22.81%, respectively compared to untreated control KM12 2.16%. Derivatives **5d** and **7c** which revealed selective cytotoxic activity against KM12 cells in addition to apoptotic effect confirmed by annexin V-FITC staining method may serve as promising leads as apoptotic inducers in colon cancer treatment.

4. Experimental section

4.1. Chemistry

Melting points were determined with Stuart SMP3 version 5.0 apparatus and were uncorrected. FT-IR spectra were recorded on Shimadzu-FTIR spectrophotometer using KBr discs and expressed in wave number (cm^{-1}). ^{1}H and ^{13}C NMR spectra were recorded with Bruker Advance 400 spectrophotometer operating at 400 MHz and 100 MHz, respectively and a varian mercury VXR-300 spectrophotometer (300 MHz for ^{1}H) and the chemical shifts were given in δ as parts per million (ppm) downfield from tetramethylsilane (TMS) as internal standard. Elemental microanalysis was performed at the Regional Center for Mycology and Biotechnology, AL-Azhar University, Egypt. The reactions were monitored by TLC (Merck, Germany), the spots were detected by exposure to UV lamp at λ 254 nm. All reagents and solvents were purified and dried by standard techniques.

4.1.1. Compounds *1a, 1b, 2a, 2b, 3a, 3b, 4a, 4c* and *4d*

Have been prepared according to the reported methods [47–51,55].

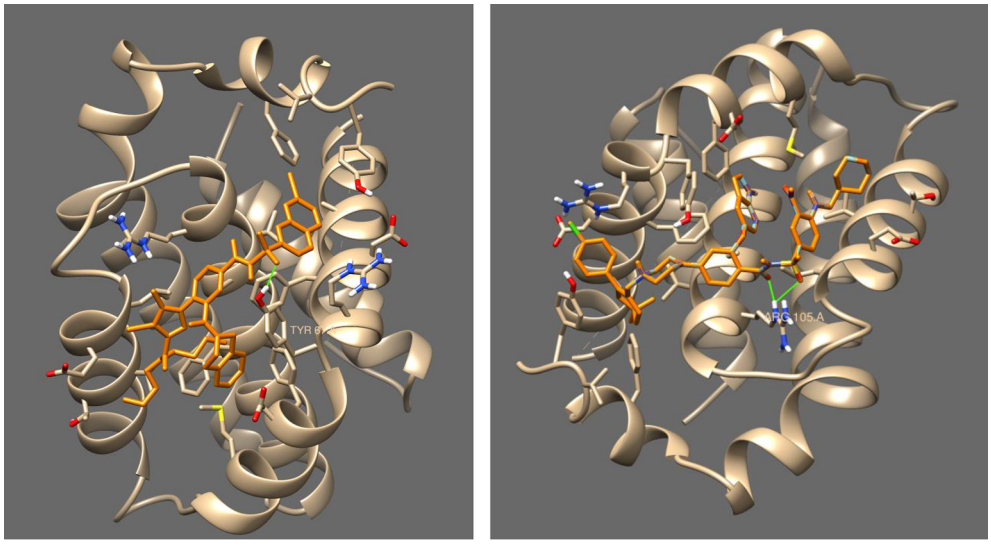

Fig. 6. The docked pose of the co-crystallized ligand 398 **A** (orange) and venetoclax **B** (orange) in the active site of Bcl-2 [PDB ID: 4AQ3].

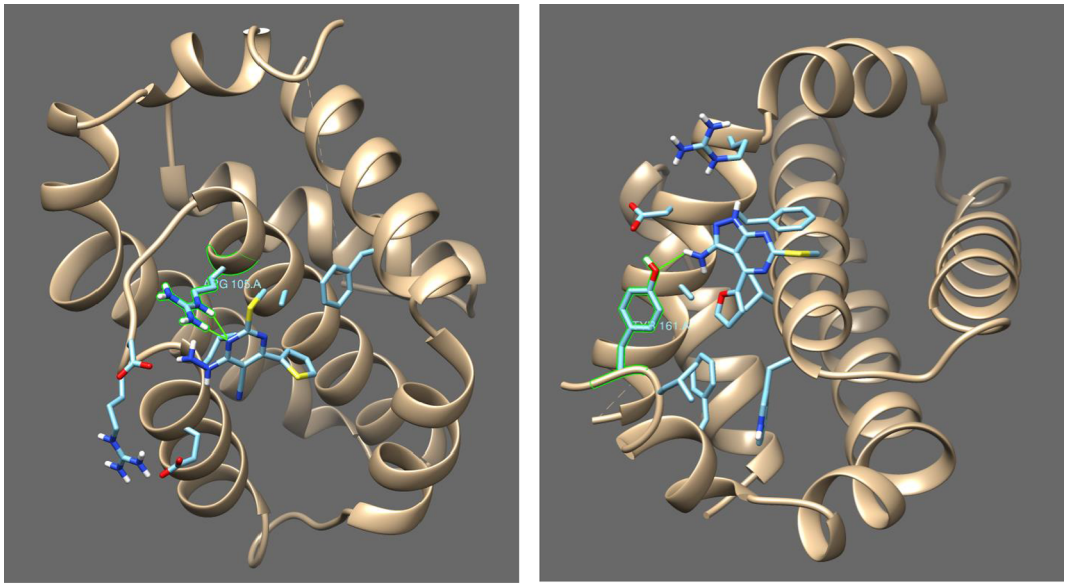

Fig. 7. The proposed binding pose for the interaction of the **5d** (A; blue) and **7c** (B; blue) in the active site of Bcl-2 [PDB ID: 4AQ3].

*4.1.2. Synthesis of 6-Chloro-4-(thiophen-2-yl)-2-thioxo-1,2-dihydropyrimidin-5-carbonitrile (**4b**)*

4-Oxo-6-(thiophen-2-yl)-2-thioxo-1,2,3,4-tetrahydropyrimidin-5-carbonitrile (**1b**) (8.5 mmol, 2 g) in a mixture of $POCl_3$ (10 mL) and PCl_5 (8.5 mmol, 1.76 g) was refluxed for 30 h. The reaction mixture was poured on ice/water and the residue was filtered off and crystallized from methanol.

Yield: 84%; Melting point: 280–282 °C; IR υ_{max}/cm^{-1}: 3440 (NH), 3113 (CH aromatic), 3000 (CH aliphatic) 2228 (CN). ^{1}H NMR (300 MHz, DMSO-d_6) δ 7.30 (dd, 1H, thiophene C4-H, J = 4.2, 5.1 Hz), 7.98 (d, 1H, thiophene C3-H, J = 4.2 Hz), 8.08 (d, 1H, thiophene C5-H, J = 5.1 Hz), 11.81 (s, 1H, NH, exchangeable with D_2O). Anal. Calcd for $C_9H_4ClN_3S_2$ (253.73): C, 42.60; H, 1.59; N, 16.56. Found: C, 42.76; H, 1.83; N, 16.82.

*4.1.3. Synthesis of compounds **5a-d***

To a solution of **4a-d** (1 mmol) in methanol (10 mL), hydrazine hydrate 99% (3 mmol) was added dropwise. The reaction mixture was stirred for 5 h at room temperature then the precipitate was filtered, washed and crystallized from methanol.

*4.1.3.1. 4-(Furan-2-yl)-6-hydrazinyl-2-thioxo-1,2-dihydropyrimidin-5-carbonitrile (**5a**).* Yield: 82%; Melting point: > 300 °C; IR υ_{max}/cm^{-1}: 3350–3194 (NH, NH_2), 3140 (CH aromatic), 2193 (CN). ^{1}H NMR (400 MHz, DMSO-d_6) δ 6.73 (dd, 1H, furan C4-H, J = 3.56, 1.72 Hz), 7.19–7.39 (s, br., 4H, NH pyrimidine and NHNH$_2$, exchangeable with D_2O), 7.43 (d, 1H, furan C3-H, J = 3.56 Hz), 7.98 (d, 1H, furan C5-H, J = 1.0 Hz). Anal. Calcd for $C_9H_7N_5OS$ (233.25): C, 46.34; H, 3.02; N, 30.03. Found: C, 46.13; H, 3.25; N, 30.21.

*4.1.3.2. 6-Hydrazinyl-4-(thiophen-2-yl)-2-thioxo-1,2-dihydropyrimidin-5-carbonitrile (**5b**).* Yield: 76%; Melting point: 169–171 °C; IR υ_{max}/cm^{-1}: 3332–3146 (NH, NH_2), 3099 (CH aromatic), 2209 (CN). ^{1}H NMR (400 MHz, DMSO-d_6) δ 5.19–6.76 (s, br., 4H, NH pyrimidine and NHNH$_2$, exchangeable with D_2O), 7.04–7.97 (m, 3H, aromatic-H). ^{13}C NMR (100 MHz, DMSO-d_6) δ 75.30, 119.03, 129.71, 132.27, 132.56, 141.84, 154.99, 155.62, 185.78. Anal. Calcd for $C_9H_7N_5S_2$ (249.32): C, 43.36; H, 2.83; N, 28.09. Found: C, 43.59; H, 3.01; N, 28.41.

*4.1.3.3. 4-(Furan-2-yl)-6-hydrazinyl-2-(methylthio)pyrimidin-5-carbonitrile (**5c**).* Yield: 86%; Melting point: 181–183 °C; IR υ_{max}/cm^{-1}: 3315–3265 (NH, NH_2), 3133 (CH aromatic), 2921 (CH aliphatic), 2208 (CN). ^{1}H NMR (400 MHz, DMSO-d_6) δ 2.54 (s, 3H, SCH$_3$), 3.42–3.50 (s, br., 3H, NHNH$_2$, exchangeable with D_2O), 6.76 (dd, 1H, furan C4-H, J = 3.52, 1.72 Hz), 7.43 (d, 1H, furan C3-H, J = 3.4 Hz), 8.04 (d, 1H, furan C5-H, J = 0.88 Hz). ^{13}C NMR (100 MHz, DMSO-d_6) δ 14.12, 77.54, 112.71, 113.19, 115.90, 116.44, 147.69, 150.04, 161.89, 162.95, 174.08. Anal. Calcd for $C_{10}H_9N_5OS$ (247.28): C, 48.57; H, 3.67; N, 28.32. Found: C, 48.34; H, 3.80; N, 28.65.

*4.1.3.4. 4-Hydrazinyl-2-(methylthio)-6-(thiophen-2-yl)pyrimidin-5-carbonitrile (**5d**).* Yield: 87%; Melting point: 260–262 °C; IR υ_{max}/cm^{-1}: 3309–3170 (NH, NH_2), 3093 (CH aromatic), 2970 (CH aliphatic), 2210 (CN). ^{1}H NMR (400 MHz, DMSO-d_6) δ 2.54 (s, 3H, SCH$_3$), 4.76 (s, 2H, NH$_2$, exchangeable with D_2O), 7.23 (m, 1H, thiophene C4-H), 7.90 (d, 1H, thiophene C3-H, J = 4.84 Hz), 8.18 (d, 1H, thiophene C5-H, J = 2.52 Hz), 9.39 (s, 1H, NH, exchangeable with D_2O). ^{13}C NMR (100 MHz, DMSO-d_6) δ 14.09, 77.64, 116.92, 129.28, 130.68, 133.09, 140.71, 162.10, 173.84. Anal. Calcd for $C_{10}H_9N_5S_2$ (263.34): C, 45.61; H, 3.44; N, 26.59. Found: C, 45.89; H, 3.61; N, 26.78.

*4.1.4. Synthesis of compounds **6a-h***

A mixture of **2a, b** (5 mmol), the appropriate chalcone (5 mmol) and sodium hydroxide (5 mmol, 0.2 g) in absolute ethanol (30 mL) was refluxed for 70 h. The reaction mixture was filtered on hot then the filtrate was poured on ice\water, neutralized with acetic acid and left for 24 h at room temperature. The residue was filtered off and the crude product was crystallized from methanol.

*4.1.4.1. 2-(3,5-Diphenyl-4,5-dihydro-1H-pyrazol-1-yl)-4-(furan-2-yl)-6-oxo-1,6-dihydropyrimidin-5-carbonitrile (**6a**).* Yield: 61%; Melting point: 267–269 °C; IR υ_{max}/cm^{-1}: 3367 (NH), 3032 (CH aromatic), 2993 (CH aliphatic), 2218 (CN), 1658 (C=O). ^{1}H NMR (400 MHz, DMSO-d_6) δ 3.40 (dd, 1H, C4-H$_A$ pyrazoline, J_{AX} = 4.96 Hz, J_{AM} = 18.28 Hz), 3.98 (dd, 1H, C4-H$_M$ pyrazoline, J_{MX} = 11.52 Hz, J_{MA} = 18.28 Hz), 5.77 (dd, 1H, C5-H$_X$ pyrazoline, J_{XA} = 4.96, J_{XM} = 11.52), 6.71–8.18 (m, 13H, aromatic H), 12.27 (s, 1H, NH, exchangeable with D_2O). ^{13}C NMR (100 MHz, DMSO-d_6) δ 40.20, 62.34, 100.08, 113.05, 113.18, 116.25, 125.56, 125.85, 126.36, 127.04, 127.79, 128.14, 128.59, 129.01, 129.10, 129.14, 129.28, 130.40, 130.95, 134.67, 147.00, 156.94, 157.97, 172.50. Anal. Calcd for $C_{24}H_{17}N_5O_2$ (407.42): C, 70.75; H, 4.21; N, 17.19. Found: C, 70.62; H, 4.36; N, 17.32.

4.1.4.2. 2-(5-(4-Chlorophenyl)-3-phenyl-4,5-dihydro-1H-pyrazol-1-yl)-4-(furan-2-yl)-6-oxo-1,6-dihydropyrimidin-5-carbonitrile ***(6b)***. Yield: 72%; Melting point: > 300 °C; IR υ_{max}/cm^{-1}: 3371 (NH), 3024 (CH aromatic), 2985 (CH aliphatic), 2218 (CN), 1651 (C=O). ^{1}H NMR (400 MHz, DMSO-d_6) δ 3.33 (dd, 1H, C4-H$_A$ pyrazoline, J_{AX} = 4.72 Hz, J_{AM} = 17.48 Hz), 3.97 (dd, 1H, C4-H$_M$ pyrazoline, J_{MX} = 11.52 Hz, J_{MA} = 17.48 Hz), 5.79 (dd, 1H, C5-H$_X$ pyrazoline, J_{XA} = 4.72, J_{XM} = 11.52), 6.73–8.16 (m, 12H, aromatic H), 12.35 (s, 1H, NH, exchangeable with D_2O). ^{13}C NMR (100 MHz, DMSO-d_6) δ 21.58, 40.41, 61.55, 82.68, 112.88, 115.31, 127.26, 127.51 , 128.35, 129.01, 129.08, 129.57, 130.64, 131.70, 132.15, 142.41, 146.46, 151.10, 156.92, 172.51. Anal. Calcd for $C_{24}H_{16}ClN_5O_2$ (441.87): C, 65.24; H, 3.65; N, 15.85. Found: C, 64.95; H, 3.56; N, 16.04.

4.1.4.3. 2-(5-(4-Fluorophenyl)-3-phenyl-4,5-dihydro-1H-pyrazol-1-yl)-4-(furan-2-yl)-6-oxo-1,6-dihydropyrimidin-5-carbonitrile ***(6c)***. Yield: 74%; Melting point: > 300 °C; IR υ_{max}/cm^{-1}: 3367 (NH), 3055 (CH aromatic), 2908 (CH aliphatic), 2218 (CN), 1658 (C=O). ^{1}H NMR (400 MHz, DMSO-d_6) δ 3.37 (dd, 1H, C4-H$_A$ pyrazoline, J_{AX} = 5.04 Hz, J_{AM} = 18.32 Hz), 3.98 (dd, 1H, C4-H$_M$ pyrazoline, J_{MX} = 11.68 Hz, J_{MA} = 18.32 Hz), 5.79 (dd, 1H, C5-H$_X$ pyrazoline, J_{XA} = 5.04 Hz, J_{XM} = 11.68 Hz), 6.80–8.17 (m, 12H, aromatic H), 12.36 (s, 1H, NH, exchangeable with D_2O). ^{13}C NMR (100 MHz, DMSO-d_6) δ 42.83, 61.85, 82.65, 100.07, 113.39, 115.86, 116.07, 116.50, 117.17, 127.95, 128.21, 128.57, 129.10, 130.92, 131.43, 138.49, 146.11, 150.25, 150.77, 154.06, 156.93, 160.72, 162.15, 163.14. Anal. Calcd for $C_{24}H_{16}FN_5O_2$ (425.41): C, 67.76; H, 3.79; N, 16.46. Found: C, 67.89; H, 3.50; N, 16.25.

4.1.4.4. 4-(Furan-2-yl)-2-(5-(4-methoxyphenyl)-3-phenyl-4,5-dihydro-1H-pyrazol-1-yl)-6-oxo-1,6-dihydropyrimidin-5-carbonitrile ***(6d)***. Yield: 68%; Melting point: 236–238 °C; IR υ_{max}/cm^{-1}: 3363 (NH), 3032 (CH aromatic), 2954 (CH aliphatic), 2214 (CN), 1658 (C=O). ^{1}H NMR (400 MHz, DMSO-d_6) δ 3.35 (dd, 1H, C4-H$_A$ pyrazoline, J_{AX} = 4.64 Hz, J_{AM} = 18.28 Hz), 3.7 (s, 3H, OCH$_3$), 3.95 (dd, 1H, C4-H$_M$ pyrazoline, J_{MX} = 11.36 Hz, J_{MA} = 18.28 Hz), 5.74 (dd, 1H, C5-H$_X$ pyrazoline, J_{XA} = 4.64, J_{XM} = 11.36), 6.75–8.18 (m, 12H, aromatic H), 12.31 (s, 1H, NH, exchangeable with D_2O). ^{13}C NMR (100 MHz, DMSO-d_6) δ 40.21, 55.54, 61.99, 82.37, 113.39, 114.51, 114.51, 114.67, 116.53, 126.80, 126.92, 127.66, 127.95, 128.19, 128.56, 130.27, 131.41, 134.21, 147.40, 150.67, 153.91, 156.99, 158.23, 159.16, 162.13. Anal. Calcd for $C_{25}H_{19}N_5O_3$ (437.45): C, 68.64; H, 4.38; N, 16.01. Found: C, 68.77; H, 4.20; N, 16.28.

4.1.4.5. 2-(3,5-Diphenyl-4,5-dihydro-1H-pyrazol-1-yl)-6-oxo-4-(thiophen-2-yl)-1,6-dihydropyrimidin-5-carbonitrile ***(6e)***. Yield: 64%; Melting point: 253–255 °C; IR υ_{max}/cm^{-1}: 3436 (NH), 3025 (CH aromatic), 2929 (CH aliphatic), 2209 (CN), 1644 (C=O). ^{1}H NMR (400 MHz, DMSO-d_6) δ 3.40 (dd, 1H, C4-H$_A$ pyrazoline, J_{AX} = 4.44 Hz, J_{AM} = 18.36 Hz), 4.01 (dd, 1H, C4-H$_M$ pyrazoline, J_{MX} = 11.68 Hz, J_{MA} = 18.36 Hz), 5.77 (dd, 1H, C5-H$_X$ pyrazoline, J_{XA} = 4.44, J_{XM} = 11.68), 7.22–8.47 (m, 13H, aromatic H), 12.44 (s, 1H, NH, exchangeable with D_2O). ^{13}C NMR (100 MHz, DMSO-d_6) δ 40.21, 62.85, 82.60, 100.09, 117.78, 125.56, 126.33, 127.69, 128.15, 128.26, 129.13, 129.27, 130.88, 131.18, 131.52, 134.32, 135.62, 140.71, 142.04, 150.28, 158.50, 161.63. Anal. Calcd for $C_{24}H_{17}N_5OS$ (423.49): C, 68.07; H, 4.05; N, 16.54. Found: C, 67.84; H, 3.90; N, 16.33.

4.1.4.6. 2-(5-(4-Chlorophenyl)-3-phenyl-4,5-dihydro-1H-pyrazol-1-yl)-6-oxo-4-(thiophen-2-yl)-1,6-dihydropyrimidin-5-carbonitrile ***(6f)***. Yield: 73%; Melting point: 232–234 °C; IR υ_{max}/cm^{-1}: 3433 (NH), 3066 (CH aromatic), 2924 (CH aliphatic), 2210 (CN), 1651 (C=O). ^{1}H NMR (400 MHz, DMSO-d_6) δ 3.35 (dd, 1H, C4-H$_A$ pyrazoline, J_{AX} = 4.8 Hz, J_{AM} = 18.28 Hz), 4.00 (dd, 1H, C4-H$_M$ pyrazoline, J_{MX} = 11.52 Hz, J_{MA} = 18.28 Hz), 5.78 (dd, 1H, C5-H$_X$ pyrazoline, J_{XA} = 4.8, J_{XM} = 11.52), 7.22–8.12 (m, 12H, aromatic H), 13.43 (s, 1H, NH, exchangeable with D_2O). ^{13}C NMR (100 MHz, DMSO-d_6) δ 40.20, 56.28, 87.29, 100.36, 116.84, 125.57, 127.24, 128.39, 129.27, 129.33, 129.81, 131.97, 135.07, 139.89, 158.91, 161.08, 162.55. Anal. Calcd for $C_{24}H_{16}ClN_5OS$ (457.93): C, 62.95; H, 3.52; N, 15.29. Found: C, 62.74; H, 3.39; N, 15.48.

4.1.4.7. 2-(5-(4-Fluorophenyl)-3-phenyl-4,5-dihydro-1H-pyrazol-1-yl)-6-oxo-4-(thiophen-2-yl)-1,6-dihydropyrimidin-5-carbonitrile ***(6g)***. Yield: 71%; Melting point: 234–236 °C; IR υ_{max}/cm^{-1}: 3394 (NH), 3032 (CH aromatic), 2931 (CH aliphatic), 2210 (CN), 1651 (C=O). ^{1}H NMR (400 MHz, DMSO-d_6) δ 3.33 (dd, 1H, C4-H$_A$ pyrazoline, J_{AX} = 4.72 Hz, J_{AM} = 18.32 Hz), 3.99 (dd, 1H, C4-H$_M$ pyrazoline, J_{MX} = 11.52 Hz, J_{MA} = 18.32 Hz), 5.78 (dd, 1H, C5-H$_X$ pyrazoline, J_{XA} = 4.72, J_{XM} = 11.52), 7.16–8.12 (m, 12H, aromatic H), 12.45 (s, 1H, NH, exchangeable with D_2O). ^{13}C NMR (100 MHz, DMSO-d_6) δ 40.62, 56.28, 87.29, 100.07, 116.03, 116.25, 116.83, 125.55, 127.52, 127.60, 128.33, 129.30, 129.80, 130.06, 131.97, 135.06, 139.89, 158.89, 161.07, 162.54. Calcd for $C_{24}H_{16}FN_5OS$ (441.48): C, 65.29; H, 3.65; N, 15.86. Found: C, 65.08; H, 3.50; N, 15.99.

4.1.4.8. 2-(5-(4-Methoxyphenyl)-3-phenyl-4,5-dihydro-1H-pyrazol-1-yl)-6-oxo-4-(thiophen-2-yl)-1,6-dihydropyrimidin-5-carbonitrile ***(6h)***. Yield: 64%; Melting point: 263–265 °C; IR υ_{max}/cm^{-1}: 3421 (NH), 3032 (CH aromatic), 2958 (CH aliphatic), 2210 (CN), 1651 (C=O). ^{1}H NMR (400 MHz, DMSO-d_6) δ 3.32 (dd, 1H, C4-H$_A$ pyrazoline, J_{AX} = 4.24 Hz, J_{AM} = 18.32 Hz), 3.70 (s, 3H, OCH$_3$), 3.97 (dd, 1H, C4-H$_M$ pyrazoline, J_{MX} = 11.32 Hz, J_{MA} = 18.32 Hz), 5.74 (dd, 1H, C5-H$_X$ pyrazoline, J_{XA} = 4.24, J_{XM} = 11.32), 6.89–8.14 (m, 12H, aromatic H), 12.39 (s, 1H, NH, exchangeable with D_2O). ^{13}C NMR (100 MHz, DMSO-d_6) δ 40.62, 55.64, 65.73, 87.10, 114.55, 116.91, 125.53, 126.92, 127.77, 128.11, 128.24, 129.22, 129.84, 130.07, 131.87, 132.01, 135.00, 135.64, 140.03, 152.86, 158.43, 158.59, 159.46, 161.12, 162.58. Anal. Calcd for $C_{25}H_{19}N_5O_2S$ (453.52): C, 66.21; H, 4.22; N, 15.44. Found: C, 66.37; H, 4.48; N, 15.71.

4.1.5. Synthesis of compounds ***7a-d***

A solution of **5a-d** (4 mmol) in absolute ethanol (20 mL) and Conc. HCl (1 mL) was was heated under reflux for 12 h. The reaction mixture was cooled, neutralized with conc. Ammonia solution. The precipitate was filtered and washed with ethanol and crystallized from ethanol.

4.1.5.1. 3-Amino-4-(furan-2-yl)-1H-pyrazolo[3,4-d]pyrimidin-6(7H)-thione ***(7a)***. Yield: 78%; Melting point: > 300 °C; IR υ_{max}/cm^{-1}: 3460–3243 (NH, NH$_2$), 3100 (CH aromatic). ^{1}H NMR (400 MHz, DMSO-d_6) δ 5.92 (s, 2H, NH$_2$, exchangeable with D_2O), 6.68–8.32 (m, 4H, aromatic 3H and NH pyrimidine, exchangeable with D_2O), 12.27 (s, 1H, NH pyrazole, exchangeable with D_2O). Anal. Calcd for $C_9H_7N_5OS$ (233.25): C, 46.34; H, 3.02; N, 30.03. Found: C, 46.50; H, 3.17; N, 30.26.

4.1.5.2. 3-Amino-4-(thiophen-2-yl)-1H-pyrazolo[3,4-d]pyrimidin-6(7H)-thione ***(7b)***. Yield: 82%; Melting point: 265–267 °C; IR υ_{max}/cm^{-1}: 3401–3205 (NH, NH$_2$), 3103 (CH aromatic). ^{1}H NMR (400 MHz, DMSO-d_6) δ 5.38 (s, 2H, NH$_2$, exchangeable with D_2O), 6.39 (s, 1H, NH pyrimidine, exchangeable with D_2O), 7.27 (m, 1H, thiophene C4-H), 7.87 (dd, 1H, thiophene C3-H, J = 1.2, 5.1 Hz), 8.34 (d, 1H, thiophene C5-H, J = 3.6 Hz), 12.77 (s, 1H, NH pyrazole, exchangeable with D_2O). Anal. Calcd for $C_9H_7N_5S_2$ (249.32): C, 43.36; H, 2.83; N, 28.09. Found: C, 43.2; H, 3.09; N, 28.41.

4.1.5.3. 4-(Furan-2-yl)-6-(methylthio)-1H-pyrazolo[3,4-d]pyrimidin-3-amine ***(7c)***. Yield: 89%; Melting point: 233–235 °C; IR υ_{max}/cm^{-1}: 3373–3288 (NH, NH$_2$), 3190 (CH aromatic), 2924 (CH aliphatic). ^{1}H NMR (400 MHz, DMSO-d_6) δ 2.72 (s, 3H, SCH$_3$), 5.84 (s, 2H, NH$_2$, exchangeable with D_2O), 6.80 (dd, 1H, furan C4-H, J = 1.72, 3.52 Hz),

7.49 (m, 1H, furan C3-H), 8.09 (dd, 1H, furan C5-H, J = 0.84, 25 Hz), 12.48 (s, 1H, NH, exchangeable with D_2O). ^{13}C NMR (100 MHz, DMSO-d_6) δ 14.10, 98.59, 129.40, 132.30, 132.84, 141.50, 148.51, 154.35, 156.43, 167.97. Anal. Calcd for $C_{10}H_9N_5OS$ (247.28): C, 48.57; H, 3.67; N, 28.32. Found: C, 48.79; H, 3.81; N, 28.04.

*4.1.5.4. 6-(Methylthio)-4-(thiophen-2-yl)-1H-pyrazolo[3,4-d]pyrimidin-3-amine (**7d**)*. Yield: 92%; Melting point: 253–255 °C; IR υ_{max}/cm^{-1}: 3371–3190 (NH, NH_2), 3082 (CH aromatic), 2997 (CH aliphatic). ^1H NMR (400 MHz, DMSO-d_6) δ 2.56 (s, 3H, SCH_3), 5.35 (s, 2H, NH_2, exchangeable with D_2O), 7.30 (s, 1H, thiophene C4-H), 7.89 (d, 1H, thiophene C3-H, J = 3.52 Hz), 8.34 (s, 1H, thiophene C5-H), 12.63 (s, 1H, NH, exchangeable with D_2O). ^{13}C NMR (100 MHz, DMSO-d_6) δ 14.11, 98.58, 129.39, 132.29, 132.84, 141.50, 154.37, 156.45, 163.19, 167.98. Anal. Calcd for $C_{10}H_9N_5S_2$ (263.34): C, 45.61; H, 3.44; N, 26.59. Found: C, C, 45.68; H, 3.58; N, 26.87.

*4.1.6. Synthesis of compounds **8a-f***

To a solution of **7c** or **7d** (4 mmol) in dry pyridine (10 mL), the appropriate aryl sulfonyl chloride (4 mmol) was added and heated under reflux for 12 h. The reaction mixture was cooled, poured into 10% ice cooled HCl. The precipitate was filtered and washed with methanol and crystallized from methanol.

*4.1.6.1. 4-(Furan-2-yl)-6-(methylthio)-1-(phenylsulfonyl)-1H-pyrazolo [3,4-d]pyrimidin-3-amine (**8a**)*. Yield: 72%; Melting point: 229–231 °C; IR υ_{max}/cm^{-1}: 3495, 3413 (NH_2), 3082 (CH aromatic), 2923 (CH aliphatic), 1383, 1190 (SO_2). ^1H NMR (300 MHz, DMSO-d_6) δ 2.65 (s, 3H, SCH_3), 6.60 (s, 2H, NH_2, exchangeable with D_2O), 6.79–8.15 (m, 8H, aromatic H). ^{13}C NMR (100 MHz, DMSO-d_6) δ 14.40, 100.87, 113.54, 117.75, 127.72, 128.78, 130.15, 135.23, 137.23, 148.89, 149.87, 150.71, 151.50, 158.77, 171.26. Anal. Calcd for $C_{16}H_{13}N_5O_3S_2$ (387.44): C, 49.60; H, 3.38; N, 18.08. Found: C, 49.51; H, 3.47; N, 18.25.

*4.1.6.2. 4-(Furan-2-yl)-6-(methylthio)-1-tosyl-1H-pyrazolo[3,4-d] pyrimidin-3-amine (**8b**)*. Yield: 79%; Melting point: 193–195 °C; IR υ_{max}/cm^{-1}: 3472, 3390 (NH_2), 3052 (CH aromatic), 2927 (CH aliphatic), 1387, 1188 (SO_2). ^1H NMR (300 MHz, DMSO-d_6) δ 2.34 (s, 3H, CH_3), 2.65 (s, 3H, SCH_3), 6.58 (s, 2H, NH_2, exchangeable with D_2O), 6.79 (dd, 1H, furan C4-H, J = 1.5, 3.3 Hz), 7.40 (d, 2H, aromatic-H, J = 7.8 Hz), 7.55 (dd, 1H, furan C3-H, J = 0.9, 3.6 Hz), 7.78 (d, 2H, aromatic-H, J = 8.4 Hz), 8.14 (dd, 1H, furan C5-H, J = 1.5, 0.6 Hz). ^{13}C NMR (100 MHz, DMSO-d_6) δ 14.39, 21.58, 100.84, 113.54, 117.73, 127.40, 127.77, 129.79, 130.56, 134.32, 146.08, 148.88, 149.83, 150.72, 151.41, 158.70, 171.18. Anal. Calcd for $C_{17}H_{15}N_5O_3S_2$ (401.46): C, 50.86; H, 3.77; N, 17.44. Found: C, 51.18; H, 3.89; N, 17.68.

*4.1.6.3. 1-((4-Chlorophenyl)sulfonyl)-4-(furan-2-yl)-6-(methylthio)-1H-pyrazolo[3,4-d]pyrimidin-3-amine (**8c**)*. Yield: 69%; Melting point: 209–211 °C; IR υ_{max}/cm^{-1}: 3480–3298 (NH_2), 3110 (CH aromatic), 2927 (CH aliphatic), 1388, 1184 (SO_2). ^1H NMR (300 MHz, DMSO-d_6) δ 2.66 (s, 3H, SCH_3), 6.60 (s, 2H, NH_2, exchangeable with D_2O), 6.80–8.16 (m, 7H, aromatic H). ^{13}C NMR (100 MHz, DMSO-d_6) δ 14.21, 101.00, 113.38, 113.56, 117.82, 129.54, 129.90, 135.90, 140.27, 148.94, 149.91, 150.71, 151.72, 156.43, 169.19, 171.38. Anal. Calcd for $C_{16}H_{12}ClN_5O_3S_2$ (421.88): C, 45.55; H, 2.87; N, 16.60. Found: C, 45.31; H, 3.04; N, 16.89.

*4.1.6.4. 6-(Methylthio)-1-(phenylsulfonyl)-4-(thiophen-2-yl)-1H-pyrazolo [3,4-d]pyrimidin-3-amine (**8d**)*. Yield: 75%; Melting point: 177–179 °C; IR υ_{max}/cm^{-1}: 3443, 3294 (NH_2), 3092 (CH aromatic), 2925 (CH aliphatic), 1373, 1189 (SO_2). ^1H NMR (300 MHz, DMSO-d_6) δ 2.65 (s, 3H, SCH_3), 6.0 (s, 2H, NH_2, exchangeable with D_2O), 7.25–8.11 (m, 8H, aromatic H). ^{13}C NMR (100 MHz, DMSO-d_6) δ 14.30, 102.36, 127.51, 127.81, 129.44, 129.50, 129.71, 130.22, 133.80, 135.34, 137.24, 139.74, 152.24, 155.47, 158.48, 171.14. Anal. Calcd for $C_{16}H_{13}N_5O_2S_3$ (403.50): C, 47. 63; H, 3.25; N, 17.36. Found: C, 47.44; H, 3.42; N, 17.58.

*4.1.6.5. 6-(Methylthio)-4-(thiophen-2-yl)-1-tosyl-1H-pyrazolo[3,4-d] pyrimidin-3-amine (**8e**)*. Yield: 87%; Melting point: 185–187 °C; IR υ_{max}/cm^{-1}: 3436, 3288 (NH_2), 3207 (CH aromatic), 2923 (CH aliphatic), 1383, 1190 (SO_2). ^1H NMR (300 MHz, DMSO-d_6) δ 2.35 (s, 3H, CH_3), 2.65 (s, 3H, SCH_3), 6.08 (s, 2H, NH_2, exchangeable with D_2O), 7.26 (dd, 1H, thiophene C4-H, J = 3.9, 4.8 Hz), 7.41 (d, 2H, aromatic-H, J = 8.4 Hz), 7.82 (d, 2H, aromatic-H, J = 8.4 Hz), 7.93 (dd, 1H, thiophene C3-H, J = 0.9, 4.8 Hz), 8.10 (d, 1H, thiophene C5-H, J = 0.9 Hz). ^{13}C NMR (100 MHz, DMSO-d_6) δ 14.40, 21.60, 102.32, 127.86, 129.39, 129.71, 129.85, 130.62, 133.60, 134.33, 139.76, 141.50, 148.42, 152.13, 155.43, 167.99, 171.06. Anal. Calcd for $C_{17}H_{15}N_5O_2S_3$ (417.53): C, 48.90; H, 3.62; N, 16.77. Found: C, 49.13; H, 3.78; N, 17.01.

*4.1.6.6. 1-((4-Chlorophenyl)sulfonyl)-6-(methylthio)-4-(thiophen-2-yl)-1H-pyrazolo[3,4-d]pyrimidin-3-amine (**8f**)*. Yield: 77%; Melting point: 174–176 °C; IR υ_{max}/cm^{-1}: 3390, 3286 (NH_2), 3087 (CH aromatic), 2926 (CH aliphatic), 1384, 1184 (SO_2). ^1H NMR (300 MHz, DMSO-d_6) δ 2.65 (s, 3H, SCH_3), 6.1 (s, 2H, NH_2, exchangeable with D_2O), 7.27–8.11 (m, 7H, aromatic H). ^{13}C NMR (100 MHz, DMSO-d_6) δ 14.26, 102.47, 129.73, 129.90, 130.46, 130.48, 133.67, 133.83, 138.36, 139.70, 140.39, 152.46, 155.53, 158.56, 171.26. Anal. Calcd for $C_{16}H_{12}ClN_5O_2S_3$ (437.95): C, 43.88; H, 2.76; N, 15.99. Found: C, 44.20; H, 2.89; N, 16.24.

4.2. Biological screening

4.2.1. Preliminary in vitro anticancer screening

The cytotoxicity assays for the synthesized compounds were performed by the National Cancer Institute (NCI), Germantown MD, USA, under the Development Therapeutic Program (DTP) on a panel of 60 tumor cell lines at a single high dose of 10 μM. Data were reported as % growth inhibition of treated cells.

4.2.2. MTT cytotoxicity assay

To determine the IC_{50} of the tested compounds, MTT assay was adopted. The basic element is 3-[4,5-dimethylthiazol-2-yl]-2,5-diphenyl tetrazolium bromide (MTT). The assay depends on mitochondrial dehydrogenase enzyme produced from the viable cells and its ability to open tetrazolium ring leading to change in color of MTT solution from yellow to purple due to formazan crystals formation [56]. Cells were seeded at a density of 6000 per well in 96-well microtiter plates and incubated for 72 h. Cells were treated with five dilutions of the tested compounds (100, 10, 1.0, 0.1 and 0.01 μM) for 72 h. After that, cells were stained with MTT solution (0.5 mg/mL) at 37 °C. DMSO was added to each well to solubilize the intracellular formazan crystals. Absorbance was measured using a spectrophotometer at a wavelength of 570 nm using a back ground absorbance at 690 nm. The cell viability curves were plotted and the IC_{50} (concentration required to inhibit 50% of cell growth) values were determined.

4.2.3. Caspase 3/9 assay

Colon (KM12) cancer cells were treated with **5d** (1.73 μM) or **7c** (1.21 μM). The cells were trypsinized, rinsed with PBS and centrifuged. Subsequently, the cells were harvested, suspended in 1 mL PBS, frozen at < -20 °C and thawed with gentle mixing. This cycle of freeze/thraw was repeated for three times and centrifuged for 10 min to purify from

cell debris. Caspase 3/9 human kit is a solid phase sandwich Enzyme Linked Immuno-Sorbent Assay (ELISA). The wells of the microtiter strips provided were coated with a monoclonal specific antibody for human target caspases. Samples and unknowns were pipetted into these wells and then a rabbit antibody specific for human target caspases were added to the wells. Through the first incubation, the human target caspases 3/9 bind to the immobilized (capture) antibody and the specific active caspase 3/9 antibody served as a detection of antibody by binding to the immobilized active caspase 3/9 proteins. After the first incubation and washing to remove excess protein, a horseradish peroxidase-labeled anti-Rabbit IgG (anti-rabbit IgG HRP) was added. After a third incubation and washing to remove all excess anti-rabbit IgG HRP, a substrate solution was added to produce a colored product as a result of interaction with the bound enzyme. The intensity of the color is directly proportional to the concentration of human active caspase 3/9 in the original specimen [57].

4.2.4. Evaluation of Bax and Bcl-2 expressions

Total RNA was extracted from at least 1×10^6 cells using RNeasy Mini-spin column kit RNeasy RNA extraction kit (Qiagen). A reaction mixture (50 μL) was prepared according to the following recipe: 2X SYBR® Green RT-PCR Reaction Mix (25 μL); Forward primer (10 μM) (1.5 μL); Reverse primer (10 μM) (1.5 μL); Nuclease-free H_2O; RNA template (1 pg to 100 ng total RNA); iScript Reverse Transcriptase for One-Step RT-PCR (1 μL).

Amplification was performed using a real-time thermal detection system (Rotorgene) as follows: cDNA synthesis: 10 min at 50 °C; iScript Reverse transcriptase inactivation: 95 °C (5 min); PCR cycling and detection 45 cycles: 95 °C (10 *sec*); 55 °C (30 *sec*) then data collection step and Melt curve analysis [58].

The gene expression fold values were calculated using 2̂(-delta delta CT) method for data analysis of quantitative real time polymerase chain reaction [59]

4.2.5. In vitro Bcl-2 inhibition assay

The Bcl-2 inhibition assay was performed at Confirmatory diagnostic unit, VACSERA, Egypt using Bcl-2 TR-FRET Assay Kit- BPS Bioscience (Catalog # 50222) and protocol [60]. All samples and controls were tested in duplicate. 1x BCL TR-FRET Assay Buffer was prepared by dilution of 3x BCL TR-FRET Assay Buffer (one part) with distilled water (2 parts). Anti-His Tb labeled donor and Dye labeled acceptor were 100-fold diluted in 1x BCL TR-FRET Assay Buffer. In each well, 5 μL of both Anti-His Tb labeled donor and Dye labeled acceptor were added. In "Test inhibitor" labeled wells, 2 μL of inhibitor solution was added while in "negative control" and "positive control" wells 2 μL of the inhibitor buffer was added.

Bcl-2 peptide ligand was 40 fold diluted using 1x BCL TR-FRET Assay Buffer. 5 μL of the diluted Bcl-2 peptide ligand was added in positive control and test inhibitor wells while 5 μL of 1x BCL TR-FRET Assay Buffer was added to the negative control wells.

The reaction was initiated by adding 3 μL of diluted Bcl-2 protein to negative control, positive control and test inhibitor wells. Wells were incubated for 3 h at room temperature and the fluorescence intensity was read using microtiter plate reader of TR-FRET.

The activity percentage was calculated as follow:

$$\%Activity = (FRET_s - FRET_{neg}/FRET_p - FRET_{neg}) \times 100\%$$

where, $FRET_s$ = Sample FRET; $FRET_{neg}$ = negative control FRET and $FRET_p$ = positive control FRET.

4.2.6. Cell cycle analysis

The colon (KM12) cancer cell line was exposed to IC_{50} dose of **5d** (1.73 μM) and **7c** (1.21 μM) or to DMSO (0.002%) as a control for 24 h. Treated cells then were suspended in 0.5 mL of PBS, centrifuged, collected and fixed in ice/cold ethanol (70% v/v) for 2 h at 4 °C then, they washed with PBS, suspended using 0.1 mg/mL RNase and stained by 40 mg/mL PI. Flow cytometry analysis was performed using FACScalibur (Becton Dickinson) and Phoenix Flow Systems and Verity Software House was used in the cell cycle distributions calculations [61].

4.2.7. Apoptotic cells sub-population determination

The colon (KM12) cancer cells were exposed to IC_{50} dose of **5d** (1.73 μM) and **7c** (1.21 μM) and DMSO (0.002%) as a control for 24 h. Treated cells then were suspended in 0.5 mL of PBS, centrifuged, collected and fixed in ice/cold ethanol (70% v/v) for 2 h at 4 °C. Subsequently, the cells were washed with PBS and centrifuged. The cells were stained using a mixture of fluorescein isothiocyanate (FITC), annexin V (component no. 51-65875X) and propidium iodide (PI) and suspended in dark at 37 °C for 30 min. Flow cytometry analysis was performed using FACScalibur (Becton Dickinson) and Phoenix Flow Systems and Verity Software House was used in the cell cycle distributions calculations [62].

4.2.8. Molecular docking

AutoDock Vina [63] was used to perform docking while UCSF Chimera [64] was used in the protein crystal structure preparation [PDB ID: 4AQ3]. Gasteiger charges were applied for the protein and all ligands. The dimension of the grid box were 20 × 20 × 20 grid points and was centered on the co-crystallized ligand **398** spacing 0.375.

Acknowledgements

The authors would like to acknowledge the gratitude of the National Cancer Institute at Germantown, US for its assistance in biological screening of chemical compounds.

Declaration of Competing Interest

The authors declare that there are no conflicts of interests.

Appendix A. Supplementary material

Supplementary data to this article can be found online at https://doi.org/10.1016/j.bioorg.2020.103621.

References

[1] M. Hassan, H. Watari, A. AbuAlmaaty, Y. Ohba, N. Sakuragi, Apoptosis and Molecular Targeting Therapy in Cancer, Biomed Res. Int. 2014 (2014) 1–23, https://doi.org/10.1155/2014/150845.
[2] J. Lopez, S.W.G. Tait, Mitochondrial apoptosis: killing cancer using the enemy within, Br. J. Cancer. 112 (2015) 957–962, https://doi.org/10.1038/bjc.2015.85.
[3] S. Zaman, R. Wang, V. Gandhi, Targeting the apoptosis pathway in hematologic malignancies, Leuk Lymphoma. 55 (2014) 1980–1992, https://doi.org/10.3109/10428194.2013.855307.
[4] I.B. Shchepotin, V. Soldatenkov, R.R. Buras, R.J. Nauta, M. Shabahang, S.R. Evans, Apoptosis of human primary and metastatic colon adenocarcinoma cell lines in vitro induced by 5-fluorouracil, verapamil, and hyperthermia, Anticancer Res. 14 (1994) 1027–1031.
[5] D.A. Carson, J.M. Ribeiro, Apoptosis and disease, Lancet 341 (1993) 1251–1254.
[6] D.E. Fisher, Apoptosis in cancer therapy: crossing the threshold, Cell 78 (1994) 539–542.
[7] R.S. Wong, Apoptosis in cancer: from pathogenesis to treatment, J. Exp. Clin. Cancer Res. 30 (2011) 87, https://doi.org/10.1186/1756-9966-30-87.
[8] C.B. Thompson, Apoptosis in the pathogenesis and treatment of disease, Science 267 (1995) 1456–1462.
[9] T.V. Achenbach, E.P. Slater, H. Brummerhop, T. Bach, R. Müller, Inhibition of cyclin-dependent kinase activity and induction of apoptosis by preussin in human tumor cells, Antimicrob. Agents Chemother. 44 (2000) 2794–2801, https://doi.org/10.1128/aac.44.10.2794-2801.2000.
[10] D. Alimbetov, S. Askarova, B. Umbayev, T. Davis, D. Kipling, Pharmacological targeting of cell cycle, apoptotic and cell adhesion signaling pathways implicated in

chemoresistance of cancer cells, Int. J. Mol. Sci. 19 (2018) 1690, https://doi.org/10.3390/ijms19061690.
[11] T. Panneer Selvam, C. Richa James, P. Vijaysarathy Dniandev, S. Karyn Valzita, A mini review of pyrimidine and fused pyrimidine marketed drugs, Res. Pharm. 2 (2012) 1–9.
[12] R. Mishra, I. Tomar, Pyrimidine: the molecule of diverse biological and medicinal importance, ChemInform. 2 (2011) 758–771.
[13] R.C. Reynolds, A. Tiwari, J.E. Harwell, D.G. Gordon, B.D. Garrett, K.S. Gilbert, S.M. Schmid, W.R. Waud, R.F. Struck, Synthesis and Evaluation of Several New (2-Chloroethyl)nitrosocarbamates as Potential Anticancer Agents, J. Med. Chem. 43 (2000) 1484–1488, https://doi.org/10.1021/jm990417j.
[14] F. Focher, D. Ubiali, M. Pregnolato, C. Zhi, J. Gambino, G.E. Wright, S. Spadari, Novel nonsubstrate inhibitors of human thymidine phosphorylase, a potential target for tumor-dependent angiogenesis, J. Med. Chem. 43 (2000) 2601–2607, https://doi.org/10.1021/jm000037u.
[15] S.A.F. Rostom, H.M.A. Ashour, H.A. Abd El Razik, Synthesis and Biological Evaluation of Some Novel Polysubstituted Pyrimidine Derivatives as Potential Antimicrobial and Anticancer Agents, Arch. Pharm. Chem. Life Sci. 342 (2009) 299–310, https://doi.org/10.1002/ardp.200800223.
[16] S.F. Chowdhury, V.B. Villamor, R.H. Guerrero, I. Leal, R. Brun, S.L. Croft, J.M. Goodman, L. Maes, L.M. Ruiz-Perez, D.G. Pacanowska, I.H. Gilbert, Design, synthesis, and evaluation of inhibitors of trypanosomal and leishmanial dihydrofolate reductase, J. Med. Chem. 42 (1999) 4300–4312.
[17] Z. Guo, Y.-F. Zhu, T.D. Gross, F.C. Tucci, Y. Gao, M. Moorjani, P.J. Connors, M.W. Rowbottom, Y. Chen, R.S. Struthers, Q. Xie, J. Saunders, G. Reinhart, T.K. Chen, A.L.K. Bonneville, C. Chen, Synthesis and structure-activity relationships of 1-arylmethyl-5-aryl-6-methyluracils as potent gonadotropin-releasing hormone receptor antagonists, J. Med. Chem. 47 (2004) 1259–1271, https://doi.org/10.1021/jm030472z.
[18] S.D. Arikkatt, B. Mathew, J. Joseph, M. Chandran, A.R. Bhat, K. Krishnakumar, B.M. V, J. Joseph, M. Chandran, A.R. Bhat, Pyrimidine derivatives and its biological potential, Int. J. Org. Bioorganic Chem. 4 (2014) 1–5.
[19] K.S. Patel, K.N. Raval, S.P. Patel, A.G. Patel, S.V. Patel, P.K. Shambhubhai, P. Nivas, Review on synthesis and biological activities of pyrimidine derivatives, Int. J. Pharm. Biol. Sci. 2 (2012) 170–182.
[20] R. Kaur, P. Kaur, S. Sharma, G. Singh, S. Mehndiratta, P.M.S. Bedi, K. Nepali, Anticancer pyrimidines in diverse scaffolds: a review of patent literature., 2015.
[21] WHO | WHO Model Lists of Essential Medicines, World Health Organization, 2017.
[22] D.B. Longley, D.P. Harkin, P.G. Johnston, 5-Fluorouracil: mechanisms of action and clinical strategies, Nat. Rev. Cancer. 3 (2003) 330–338, https://doi.org/10.1038/nrc1074.
[23] N.M. Mhaidat, M. Bouklihacene, R.F. Thorne, 5-Fluorouracil-induced apoptosis in colorectal cancer cells is caspase-9-dependent and mediated by activation of protein kinase C-δ, Oncol. Lett. 8 (2014) 699–704, https://doi.org/10.3892/ol.2014.2211.
[24] M. Li, D. Ito, M. Sanada, T. Odani, M. Hatori, M. Iwase, M. Nagumo, Effect of 5-fluorouracil on G1 phase cell cycle regulation in oral cancer cell lines, Oral Oncol. 40 (2004) 63–70, https://doi.org/10.1016/S1368-8375(03)00136-2.
[25] F.A.F. Ragab, S.M. Abou-Seri, S.A. Abdel-Aziz, A.M. Alfayomy, M. Aboelmagd, Design, synthesis and anticancer activity of new monastrol analogues bearing 1,3,4-oxadiazole moiety, Eur. J. Med. Chem. 138 (2017) 140–151, https://doi.org/10.1016/j.ejmech.2017.06.026.
[26] F.M. Awadallah, G.A. Piazza, B.D. Gary, A.B. Keeton, J.C. Canzoneri, Synthesis of some dihydropyrimidine-based compounds bearing pyrazoline moiety and evaluation of their antiproliferative activity, Eur. J. Med. Chem. 70 (2013) 273–279, https://doi.org/10.1016/j.ejmech.2013.10.003.
[27] A.A. Helwa, E.M. Gedawy, S.M. Abou-Seri, A.T. Taher, A.K. El-Ansary, Synthesis and bioactivity evaluation of new pyrimidinone-5-carbonitriles as potential anticancer and antimicrobial agents, Res. Chem. Intermed. 44 (2018) 2685–2702, https://doi.org/10.1007/s11164-018-3254-y.
[28] H.A.A. Fattah, N.A. Osman, A.M. Al-Mahmoudy, N.S. El-Sayed, Synthesis of novel pyrimidine and fused pyrimidine deriatives and their in vitro antimicrobial and cytotoxic evaluation, World J. Pharm. Res. 4 (2015) 446–469.
[29] M.M. Ghorab, M.G. El-Gazzar, M.S. Alsaid, Synthesis, characterization and anti-breast cancer activity of new 4-aminoantipyrine-based heterocycles, Int. J. Mol. Sci. 15 (2014) 7539–7553, https://doi.org/10.3390/ijms15057539.
[30] M.S. Mohamed, M.M. Youns, N.M. Ahmed, Novel indolyl-pyrimidine derivatives: Synthesis, antimicrobial, and antioxidant evaluations, Med. Chem. Res. 23 (2014) 3374–3388, https://doi.org/10.1007/s00044-014-0916-1.
[31] M.M. Mohamed, A.K. Khalil, E.M. Abbass, A.M. El-Naggar, Design, synthesis of new pyrimidine derivatives as anticancer and antimicrobial agents, Synth. Commun. 47 (2017) 1441–1457, https://doi.org/10.1080/00397911.2017.1332223.
[32] M.M. Said, A.T. Taher, H.B. El-Nassan, E.A. El-Khouly, Synthesis of novel S-acyl and S-alkylpyrimidinone derivatives as potential cytotoxic agents, Res. Chem. Intermed. 42 (2016) 6643–6662, https://doi.org/10.1007/s11164-016-2487-x.
[33] L.Y. Ma, B. Wang, L.P. Pang, M. Zhang, S.Q. Wang, Y.C. Zheng, K.P. Shao, D.Q. Xue, H.M. Liu, Design and synthesis of novel 1,2,3-triazole-pyrimidine-urea hybrids as potential anticancer agents, Bioorg. Med. Chem. Lett. 25 (2015) 1124–1128, https://doi.org/10.1016/j.bmcl.2014.12.087.
[34] L.Y. Ma, L.P. Pang, B. Wang, M. Zhang, B. Hu, D.Q. Xue, K.P. Shao, B. Le Zhang, Y. Liu, E. Zhang, H.M. Liu, Design and synthesis of novel 1,2,3-triazole-pyrimidine hybrids as potential anticancer agents, Eur. J. Med. Chem. 86 (2014) 368–380, https://doi.org/10.1016/j.ejmech.2014.08.010.
[35] L.W. Zheng, L.L. Wu, B.X. Zhao, W.L. Dong, J.Y. Miao, Synthesis of novel substituted pyrazole-5-carbohydrazide hydrazone derivatives and discovery of a potent apoptosis inducer in A549 lung cancer cells, Bioorg. Med. Chem. 17 (2009) 1957–1962, https://doi.org/10.1016/j.bmc.2009.01.037.
[36] D. Shi, J. Mou, Q. Zhuang, L. Niu, N. Wu, X. Wang, Three Component one pot synthesis of 1,4-dihydropyrano[2,3-c]pyrazole derivatives in aqueous media, Synth. Commun. 34 (2004) 4557–4563, https://doi.org/10.1081/SCC-200043224.
[37] G.M. Nitulescu, C. Draghici, O.T. Olaru, New potential antitumor pyrazole derivatives: synthesis and cytotoxic evaluation, Int. J. Mol. Sci. 14 (2013) 21805–21818, https://doi.org/10.3390/ijms141121805.
[38] P.-C. Lv, H.-Q. Li, J. Sun, Y. Zhou, H.-L. Zhu, Synthesis and biological evaluation of pyrazole derivatives containing thiourea skeleton as anticancer agents, Bioorg. Med. Chem. 18 (2010) 4606–4614, https://doi.org/10.1016/j.bmc.2010.05.034.
[39] B. Yang, Y.S. Yang, N. Yang, G. Li, H.L. Zhu, Design, biological evaluation and 3D QSAR studies of novel dioxin-containing pyrazoline derivatives with thiourea skeleton as selective HER-2 inhibitors, Sci. Rep. 6 (2016) 1–12, https://doi.org/10.1038/srep27571.
[40] Y. Wang, F.X. Cheng, X.L. Yuan, W.J. Tang, J.B. Shi, C.Z. Liao, X.H. Liu, Dihydropyrazole derivatives as telomerase inhibitors: Structure-based design, synthesis, SAR and anticancer evaluation in vitro and in vivo, Eur. J. Med. Chem. 112 (2016) 231–251, https://doi.org/10.1016/j.ejmech.2016.02.009.
[41] H. Wang, J. Zheng, W. Xu, C. Chen, D. Wei, W. Ni, Y. Pan, A new series of cytotoxic pyrazoline derivatives as potential anticancer agents that induce cell cycle arrest and apoptosis, Molecules 22 (2017) 1–14, https://doi.org/10.3390/molecules22101635.
[42] R.F. George, M.A. Fouad, I.E.O. Gomaa, Synthesis and cytotoxic activities of some pyrazoline derivatives bearing phenyl pyridazine core as new apoptosis inducers, Eur. J. Med. Chem. 112 (2016) 48–59, https://doi.org/10.1016/j.ejmech.2016.01.048.
[43] G.S. Hassan, D.E. Abdel Rahman, Y.M. Nissan, E.A. Abdelmajeed, T.M. Abdelghany, Novel pyrazolopyrimidines: Synthesis, in vitro cytotoxic activity and mechanistic investigation, Eur. J. Med. Chem. 138 (2017) 565–576, https://doi.org/10.1016/j.ejmech.2017.07.003.
[44] M. El-Naggar, A. Hassan, H. Awad, M. Mady, Design, Synthesis and Antitumor Evaluation of Novel Pyrazolopyrimidines and Pyrazoloquinazolines, Molecules 23 (2018) 1249, https://doi.org/10.3390/molecules23061249.
[45] C. Karthikeyan, C. Lee, J. Moore, R. Mittal, E.A. Suswam, K.L. Abbott, S.R. Pondugula, U. Manne, N.K. Narayanan, P. Trivedi, A.K. Tiwari, IND-2, a pyrimido[1″,2″:1,5]pyrazolo[3,4-b]quinoline derivative, circumvents multi-drug resistance and causes apoptosis in colon cancer cells, Bioorg. Med. Chem. 23 (2015) 602–611, https://doi.org/10.1016/j.bmc.2014.11.043.
[46] X. Li, A. Wang, K. Yu, Z. Qi, C. Chen, W. Wang, C. Hu, H. Wu, J. Wu, Z. Zhao, J. Liu, F. Zou, L. Wang, B. Wang, W. Wang, S. Zhang, J. Liu, Q. Liu, Discovery of (R)-1-(3-(4-Amino-3-(4-phenoxyphenyl)-1H-pyrazolo[3,4-d]pyrimidin-1-yl)piperidin-1-yl)-2-(dimethylamino)ethanone (CHMFL-FLT3-122) as a Potent and Orally Available FLT3 Kinase Inhibitor for FLT3-ITD Positive Acute Myeloid Leukemia, J. Med. Chem. 58 (2015) 9625–9638, https://doi.org/10.1021/acs.jmedchem.5b01611.
[47] V.J. Ram, D.A. Vanden Berghe, A.J. Vlietinck, Chemotherapeutical agents, V. syntheses and activities of novel pyrimidines derived from 5-cyano-6-aryl-2-thiouracil, Liebigs Ann. Chem. (1987 (1987)) 797–801, https://doi.org/10.1002/jlac.198719870831.
[48] F.A. Attaby, S.M. Eldin, E.A.Z. Hanafi, Reactions of Pyrimidinonethione derivatives : synthesis of 2-arylhydrazonopyrimidin-4-one, Pyrimido[1,2-a]-l,2,4-triazine, Triazolo-[1,2-a]pyrimidine, 2-(1 -pyrazolo)pyrimidine and 2-arylhydrazonopyrimidine derivatives derivatives, Arch. Pharm. Res. 20 (1997) 620–628.
[49] E.B. Moawad, Synthesis and reactions of fused cyanopyrimidine derivatives as affecting enzymatic agents, Mansoura Sci. Bull. A Chem. 29 (2002) 29–38.
[50] N. Agarwal, P. Srivastava, S.K. Raghuwanshi, D.N. Upadhyay, S. Sinha, P.K. Shuklab, V.J. Ram, Chloropyrimidines as a new class of antimicrobial agents, Bioorg. Med. Chem. 10 (2002) 869–874, https://doi.org/10.1039/C3OB40444G.
[51] A.M. Fargualy, N.S. Habib, K.A. Ismail, A.M.M. Hassan, M.T.M. Sarg, Synthesis, biological evaluation and molecular docking studies of some pyrimidine derivatives, Eur. J. Med. Chem. 66 (2013) 276–295, https://doi.org/10.1016/j.ejmech.2013.05.028.
[52] B.L. Lampson, M.S. Davids, The Development and Current Use of BCL-2 Inhibitors for the Treatment of Chronic Lymphocytic Leukemia, Curr. Hematol. Malig. Rep. 12 (2017) 11–19, https://doi.org/10.1007/s11899-017-0359-0.
[53] C. Bodur, H. Basaga, Bcl-2 inhibitors: emerging drugs in cancer therapy, Curr. Med. Chem. 19 (2012) 1804–1820, https://doi.org/10.2174/092986712800099839.
[54] J. Mihalyova, T. Jelinek, K. Growkova, M. Hrdinka, M. Simicek, R. Hajek, Venetoclax: A new wave in hematooncology, Exp. Hematol. 61 (2018) 10–25, https://doi.org/10.1016/j.exphem.2018.02.002.
[55] I.M. Abdou, A.M. Attia, L. Strekowski, Glucopyranosides derived from 6-aryl-5-cyano-2-(methylthio) pyrimidin-4(3H)ones, Nucleosides, Nucleotides Nucleic Acids. 21 (2006) 2002.
[56] T. Mosmann, Rapid colorimetric assay for cellular growth and survival: application to proliferation and cytotoxicity assays, J. Immunol. Methods. 65 (1983) 55–63.
[57] M. Andersson, J. Sjöstrand, A. Petersen, A.K. Honarvar, J.O. Karlsson, Caspase and proteasome activity during staurosporin-induced apoptosis in lens epithelial cells, Invest. Ophthalmol. Vis. Sci. 41 (2000) 2623–2632.
[58] K.J. Livak, T.D. Schmittgen, Analysis of relative gene expression data using real-time quantitative PCR and the 2-ΔΔCT method, Methods 25 (2001) 402–408, https://doi.org/10.1006/meth.2001.1262.
[59] X. Rao, X. Huang, Z. Zhou, X. Lin, An improvement of the 2̂(-delta delta CT) method for quantitative real-time polymerase chain reaction data analysis, Biostat. Bioinforma. Biomath. 3 (2013) 71–85.
[60] P. Filippakopoulos, S. Picaud, M. Mangos, T. Keates, J.-P. Lambert, D. Barsyte-Lovejoy, I. Felletar, R. Volkmer, S. Müller, T. Pawson, A.-C. Gingras, C.H. Arrowsmith, S. Knapp, Histone recognition and large-scale structural analysis of the human bromodomain family, Cell 149 (2012) 214–231, https://doi.org/10.

1016/j.cell.2012.02.013.
[61] I. Nicoletti, G. Migliorati, M.C. Pagliacci, F. Grignani, C. Riccardi, A rapid and simple method for measuring thymocyte apoptosis by propidium iodide staining and flow cytometry, J. Immunol. Methods. 139 (1991) 271–279.
[62] I. Vermes, C. Haanen, H. Steffens-Nakken, C. Reutelingsperger, A novel assay for apoptosis. Flow cytometric detection of phosphatidylserine expression on early apoptotic cells using fluorescein labelled Annexin V, J. Immunol. Methods. 184 (1995) 39–51.
[63] O. Trott, A.J. Olson, Software news and update AutoDock Vina: Improving the speed and accuracy of docking with a new scoring function, efficient optimization, and multithreading, J. Comput. Chem. 31 (2010) 455–461, https://doi.org/10.1002/jcc.21334.
[64] E.F. Pettersen, T.D. Goddard, C.C. Huang, G.S. Couch, D.M. Greenblatt, E.C. Meng, T.E. Ferrin, UCSF Chimera - A visualization system for exploratory research and analysis, J. Comput. Chem. 25 (2004) 1605–1612, https://doi.org/10.1002/jcc.20084.